Title

Development of Empirical-Mechanistic Pavement Performance Models using Data from the Washington State PMS Database

Authors

Madanat, S M
Nakat, Ziad El
Sathaye, Nakul

Publication Date

2005-10-01

Peer reviewed

Development of Empirical-Mechanistic Pavement Performance Models using Data from the Washington State PMS Database

Final Report prepared for the California Department of Transportation through the Partnered Pavement Research Center Contract, PPRC Item 4.5

Prepared by Samer Madanat, Ziad Nakat,
and Nakul Sathaye

UC Pavement Research Center
University of California, Davis and Berkeley

UCPRC-RR-2005-5

October 2005

EXECUTIVE SUMMARY

A Pavement Management System (PMS) is a decision-support tool that aids public agencies in planning maintenance activities of their facilities. A complete PMS involves the following tasks: inspecting facilities and collecting data, predicting the deterioration of facilities through performance models, and optimizing the Maintenance, Rehabilitation, and Reconstruction (MR&R) policies over the planning horizon. Performance models are a core component of PMS. These models are also used to calibrate facility design procedures.

The main objective of this project was to develop Empirical-Mechanistic (E-M) performance models using data from Washington State's PMS databases. Four models were developed from that data:

1. A model for predicting the initiation of overlay cracking in asphalt concrete (AC) pavements
2. A model for predicting the progression of roughness for AC pavements
3. A model for predicting the initiation of cracking in portland cement concrete (PCC) pavements
4. A model for predicting the progression of roughness for portland cement concrete pavements

At the start of the project, models using pavement maintenance data from the Washington State Department of Transportation (WSDOT) and the Arizona Department of Transportation (ADOT) were attempted. The initial reasoning for using PMS data from those states is that they have very measured pavement conditions consistently over a long period of time, and they have topographic and climate regions similar to parts of California. Therefore, Caltrans could use models developed using data from those states to manage a subset of California's pavement infrastructure until the department develops the database needed to support model development. However, the research team found that the ADOT data were inappropriate for developing the type of performance models needed in this project, so only WSDOT pavement data were used.

To develop these models, the following tasks were performed:

1. The WSDOT PMS databases were mined for the most relevant variables, including pavement section structure, traffic, surface condition, and resurfacing activities. These were augmented with environmental data obtained from external data sources.
2. Appropriate functional forms were selected for the empirical models and relevant explanatory variables included.
3. Appropriate statistical modeling tools were used to calibrate (estimate) the parameters of the performance models.
4. Classical statistical tests were performed on all models to confirm the statistical significance of the various parameters and of the models as a whole.
5. Predictions were performed using the various models to confirm that they produced realistic results.

Conclusions from this research can be summarized as follows:

1. The performance models for cracking initiation and International Roughness Index (IRI) developed using the WSDOT PMS data for AC pavements or overlays are satisfactory.
2. The following explanatory variables were found to be the most relevant predictors of the number of Equivalent Single Axle Loads (ESALs) to cracking initiation (defined as five percent of the wheelpath cracked) of overlays on AC pavements:
    - The overlay thickness
    - The type of AC mix used for the overlay
    - The thickness of the underlying AC layers prior to application of the overlay
    - The existing longitudinal and alligator cracking prior to the application of the overlay
    - The base thickness and type (whether it was untreated, granular, portland cement-treated, or asphalt-treated)

- The maximum temperature during the hottest month and the minimum temperature during the coldest month (averages taken over the life of the overlay)
- The number of freeze-thaw cycles and the average precipitation

3. The following explanatory variables were found to be the most relevant predictors of the annual increment in IRI for AC pavements and overlays:

   - The IRI in the previous year
   - The number of ESALs in the subject year
   - The cumulative number of ESALs prior to the subject year
   - The base thickness
   - The total thickness of asphalt concrete (AC), including all overlays
   - The number of years since the last overlay or bituminous surface treatment
   - The type of the last MR&R activity applied to the pavement, either AC overlay, bituminous surface treatment (BST, equivalent of Caltrans aggregate seal coat), or routine maintenance
   - The minimum temperature in the coldest month (average over the life of the pavement)
   - The annual precipitation (average over the life of the pavement)

4. We did not succeed in developing models using the WSDOT PMS data for PCC pavements (crack initiation and IRI). The small number of PCC observations available in the WSDOT PMS database made it impossible to develop adequate models.

5. This research has also identified a list of variables that are recommended for collection by Caltrans. Elements of these variables are currently collected by other state departments of transportation. Appendix A lists of the variables.

6. A numerical integration procedure was developed using macros in *Microsoft Excel* to help with the application of the model used to predict cracking initiation for AC overlays. The description of this procedure appears in Appendix B.

The main recommendations contained in the report are:

1. To complete the AC pavement performance model suite, a crack progression model should be developed. The progression model should be used jointly with the crack initiation model developed in this research to predict development of cracking beyond five percent of the wheelpath cracked.

2. The completed AC pavement models (crack initiation and progression, IRI progression) should be tested on California PMS data. These data can either be collected as part of a pilot project or mined from data in the Caltrans PMS database after that database has been populated with information collected over consistently segmented sections. If the results of the tests are positive, then Caltrans can essentially use these models as temporary AC pavement performance models.

3. Once Caltrans has populated its PMS database with sufficiently extensive condition survey data, the models developed in this report can be updated with the California data by using statistical fusion procedures, such as Bayesian Updating.

4. The ultimate objective of the development of such models is to use them within an integrated Pavement Management System. The models can provide predictions to support MR&R planning at both the project and network levels. Therefore, to fully reap the benefits of its investment in this research, Caltrans should continue its efforts at modernizing its Pavement Management System.

TABLE OF CONTENTS

TABLE OF TABLES

TABLE OF FIGURES

1.0 INTRODUCTION

A Pavement Management System (PMS) is a decision-support tool that aids public agencies in planning maintenance activities of their facilities. A complete PMS involves: inspecting facilities and collecting data, predicting the deterioration of facilities through performance models, and optimizing the Maintenance, Rehabilitation and Reconstruction (MR&R) policies over the planning horizon. Performance models are a core component of a PMS. These models are also used as an input in project design procedures.

Several PMSs have been developed and applied to actual pavement networks. For example, in the first year that the Arizona Pavement Management System was implemented, it was successful in saving an estimated $14 million (fiscal year 1980–1981), one third of Arizona's maintenance budget, and $101 million in the first four years. The state of California spends an average of $350 million per year on contracted pavement maintenance and rehabilitation, and this expenditure may exceed $700 million per year in the near future. There is potential for this expense to be reduced if PMS improvements are developed and implemented.

The main objective of this project is to develop a set of Empirical-Mechanistic (E-M) performance models using data from Washington State's PMS databases. Our research team attempted to develop four performance models:

1. A model for predicting the initiation of overlay cracking in Asphalt Concrete (AC) pavements,
2. A model for predicting the progression of roughness for AC pavements,
3. A model for predicting the initiation of cracking in portland cement concrete (PCC) pavements, and
4. A model for predicting the progression of roughness for PCC pavements.

For the purpose of this project, models using pavement maintenance data from the Washington State DOT (WSDOT) and the Arizona DOT (ADOT) were attempted. The team reasoned that because Washington and Arizona contain topographic and climate regions similar to parts of California, as well as a degree of traffic similarity, the models developed for those states could be used by Caltrans to better manage a subset of California's pavement infrastructure—until the department develops its own database to

support a California-derived model development. However, when the research team found that the ADOT data were inappropriate for developing the type of performance models needed in this project, a decision was made to use only the WSDOT pavement data.

The research report describes Empirical-Mechanistic (E-M) models, which are deductive models. In E-M models, functional form and specification (choice of explanatory variables) are based on physical considerations and the model parameters (coefficients) are calibrated by using empirical data and statistical estimation procedures. This modeling approach is the only feasible one in cases where a mechanistic analysis is impossible either because the exact physical process of deterioration is poorly understood (e.g., in the case of reflection cracking of AC overlays) or too complex (e.g., roughness progression, where roughness is a measure of performance that includes the effects of several distresses).

Unlike Mechanistic-Empirical (M-E) methods, E-M models require knowledge of only a small set of variables, many of which are routinely measured in pavement condition surveys or are available from maintenance records, traffic counts, and as-built records. This makes E-M models especially suitable for network-level pavement management systems. For project-level designs, where detailed information can be collected, M-E methods are more appropriate.

This report is organized as follows: Chapter 2 presents the methodology used to develop crack initiation models for AC pavements. Chapter 3 presents the crack initiation models that were developed for AC pavements and Chapter 4 presents the IRI (International Roughness Index) progression models for AC pavements. Chapter 5 discusses our investigations of deterioration for PCC pavements. Chapter 6 summarizes our conclusions and recommendations. Appendix A provides a list of variables that are recommended for collection by Caltrans. (Elements of these variables are currently collected by other state DOTs.) Appendix B provides the numerical integration procedure used for computing both the expected ESALs-to-cracking initiation for overlays placed on AC pavements and the predictions performed in Chapter 3.

2.0 REVIEW OF METHOD USED TO DEVELOP CRACK INITIATION MODELS

In this section we will review the statistical background used in the development of Asphalt Concrete Overlay Crack Initiation models.

The initiation of pavement distress is highly variable because distress occurs at different times at various locations along a homogeneous piece of road. Therefore, the time of failure should be represented by a probability density function rather than by a point estimate. For this reason, Duration models (or Hazard Rate models) were used instead of Regression models, which only provide point estimates.

Duration/Hazard Rate models were also better suited here because they predict a survival function for the time of failure of an element or system. Moreover, point estimate models of the initiation of pavement distress lack the structure, as well as the physical significance, offered by Duration models.

In this section we will discuss the Hazard Rate Model, and then explain the different types of censoring that might occur in condition surveys, and the method to account for censoring in model estimation. We will also present an overview of two types of Duration models, the Weibull Model and the Cox Model, and explain the advantages of each.

2.1 Hazard Rate Model

Define T as the time (or Cumulative ESALs) to cracking of a pavement, where T is a random variable that takes values in the interval $(0,\infty)$. It has a cumulative distribution F(t) and a density function f(t). F(t) is given by:

$$F(t) = \int_0^t f(s)ds = \Pr ob(T \le t) \qquad \textbf{(1)}$$

The probability that cracking occurs after time t is given by the survival function:

$$S(t) = 1 - F(t) = \Pr ob(T \ge t) \qquad \textbf{(2)}$$

We define g(t) as the probability that a pavement cracks in the next small interval, Δt, given it lasts at least until time t:

$$g(t) = \Pr ob(t \le T < \mathbf{t} + \Delta \mathbf{t} \mid \mathbf{T} \ge \mathbf{t}) \qquad \textbf{(3)}$$

The instantaneous rate of change of g(t), defined as the Hazard Rate Function, h(t), is given by:

$$h(t) = \underset{\Delta t \to 0}{Lim} \frac{g(t)}{\Delta t} \qquad \textbf{(4)}$$

The hazard rate quantifies the instantaneous risk that the pavement sections crack at time t (Madanat and Mishalani 2002).

2.2 Censoring

Censoring occurs frequently in condition survey data because in most cases it is impossible or impractical to observe the complete lifetimes of all the pavement sections. A censored observation occurs when only a bound is known on the time of failure. A *complete data set* is when all failure times are known. A data set is called *censored* if there are one or more censored observations. There are several types of censoring. The most frequent type is *right censoring.* Right censoring occurs when there is one or more pavement sections for which only a lower bound is known on the lifetime. There are three special cases of right censoring that occur in practice. The first is Type I censoring, or *time censoring,* which corresponds to terminating the study at a particular time (Figure 1). Therefore, the number of failures is random in Type I censoring. Type II censoring — also called *order statistic censoring* — corresponds to terminating the study upon one of the ordered failures. Looking at Figure 2, we notice that it corresponds to a set of n = 5 items placed on a test that is terminated when r = 3 failures are observed. Thus, in Type II censoring the time to complete the test is random. The third type, *random censoring,* occurs when individual items are withdrawn from the test at any time during the study (Figure 3). Thus it is assumed in *random censoring* that the *i*th lifetime, t_i, and the *i*th censoring time, c_i, are independent random variables.

Another form of censoring is left censoring. An example of cases where left censoring occurs is in scientific applications where the resolution of the equipment is finite (observations whose magnitude is below a certain threshold are missing). Left censoring might also occur in long-lived pavements where data collection began after the pavements were constructed or when condition survey procedures were changed and new variables were collected only for a certain period of time. Data can be both left and right-censored if the conditions described above for left and right censoring both occur.

Moreover, there exists an additional type of censoring called *interval censoring,* which occurs when the lifetime falls into an interval. A case of interval censoring occurs when items are checked periodically for failure. The information known about the lifetime is thus that its failure time occurred during the interval prior to when failure was detected (Leemis 1995).

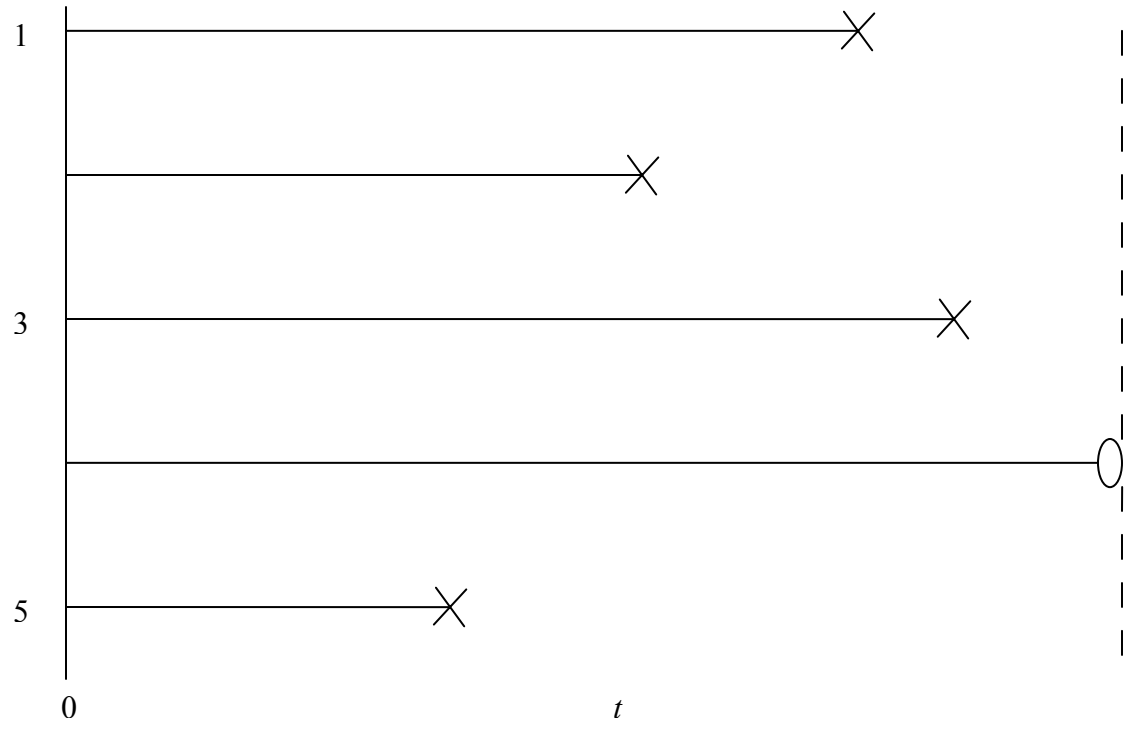

Figure 1: Type I right-censored data set with n=5 and r=4

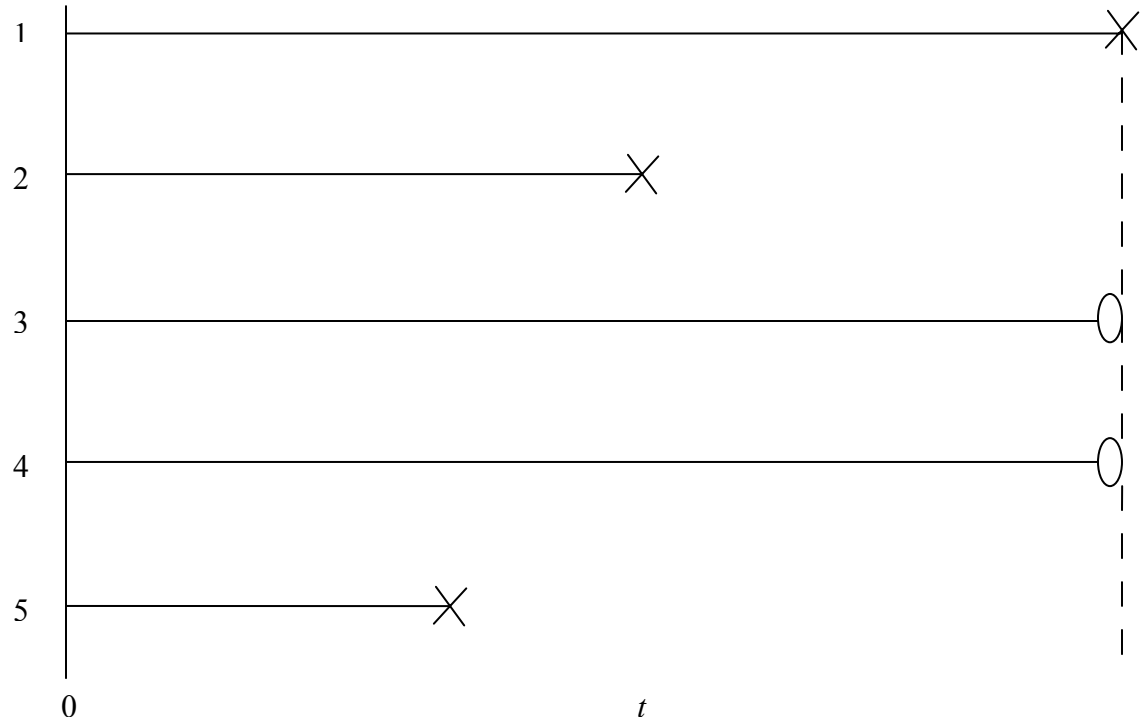

Figure 2: Type II right-censored data set with n = 5 and r = 3

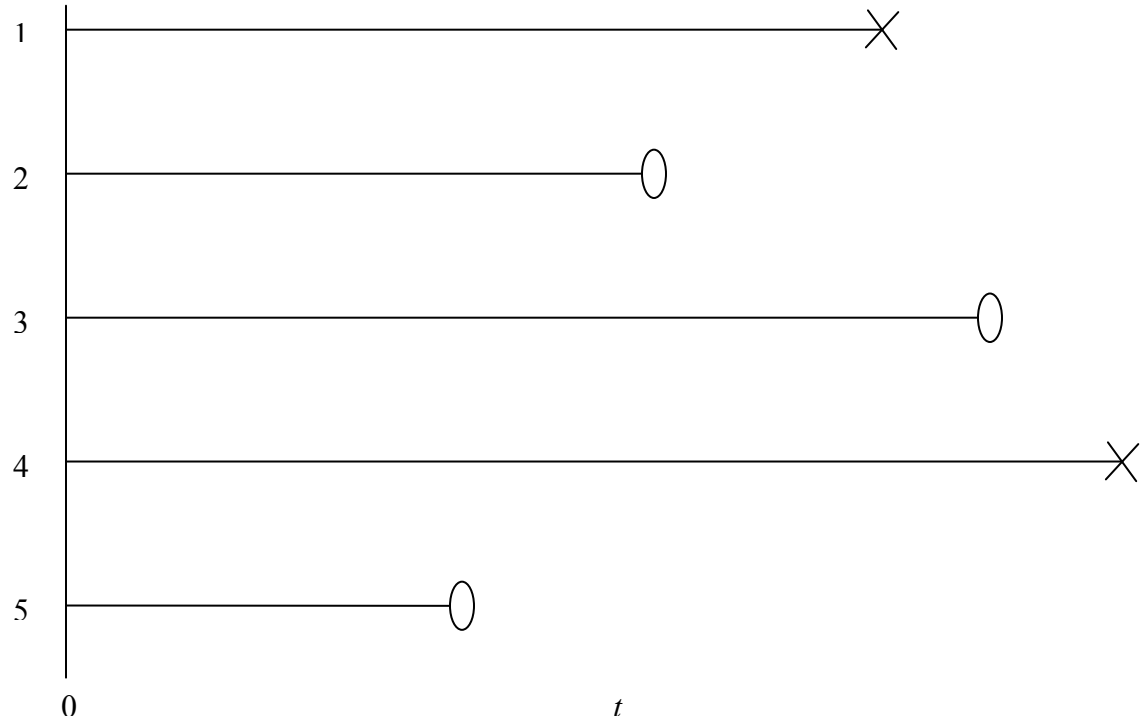

Figure 3: Type III (randomly) right-censored data set with n = 5 and r = 2

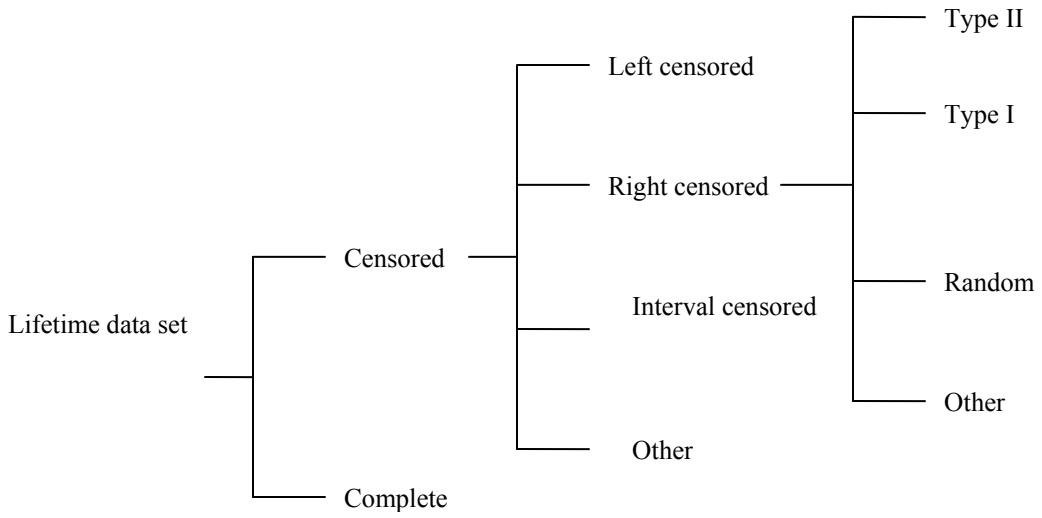

Figure 4: Lifetime data set taxonomy

In this project all our data are either interval censored or right censored. Since condition surveys occur annually, we only know that a cracked section *i* has cracked in an interval of one year $[(t_i - 1), t_i]$ where t_i is the time when section i is observed to be cracked. Sections that have not cracked by the end of the last condition survey at time C are right censored. Thus for each section *i*, we either know the interval $[(t_i - 1),t_i]$, if $t_i \leq C$ and the section has cracked, or the section has not cracked and we have right censoring with $t_i > C$.

The full likelihood function with n observations in this case is obtained by multiplying the product of the differences between the survival functions at time t_i and $t_i - 1$ for the interval-censored observations by the product of the survival functions at time t_i for the right-censored observations:

$$L = \prod_{\delta_i=1} [S(t_i) - S(t_i - 1)] \prod_{\delta_i=0} S(t_i) = \prod_{i=1}^{n} [S(t_i) - S(t_i - 1)]^{\delta_i} [S(t_i)]^{1-\delta_i} \qquad \textbf{(5)}$$

where δi is a dummy variable that takes the value 1 if observation i is interval censored and 0 if it is right censored.

To estimate the parameters, we maximize the log likelihood function:

$$\boldsymbol{l} = \mathbf{L} = \sum_{i=1}^{n} \left\{ \delta_i \log\left[S(t_i) - S(t_i - 1)\right] + (1 - \delta_i) \log\left[S(t_i)\right] \right\} \qquad \textbf{(6)}$$

For the model developed in this report, we ignored interval censoring and assumed continuous condition surveys. This simplifies the estimation of the parameters of the models, though it probably leads to a small loss of precision. The full likelihood function for such a case with n observations is given by multiplying the respective contributions of values of density function, f, for uncensored observations and values of survival function, S, for right-censored observations:

$$L = \prod_{\delta_i = 1} f(t_i) \prod_{\delta_i = 0} S(t_i) = \prod_{i=1}^{n} [f(t_i)]^{\delta_i} [S(t_i)]^{1-\delta_i} \quad \textbf{(7)}$$

where δ_i is a dummy variable that takes the value 1 if observation i is uncensored and 0 if it is right censored.

The log likelihood function is (Kalbfleisch and Prentice 2002).

$$\boldsymbol{l} = \mathbf{L} = \sum_{i=1}^{n} \left\{ \delta_i \log[f(t_i)] + (1-\delta_i) \log[S(t_i)] \right\} \quad \textbf{(8)}$$

2.3 Weibull Model

It is more general and realistic to allow the hazard rate to increase or decrease over time than to assume it to be constant (Shin 2001). Materials degrade over time and thus are more likely to follow a distribution with a strictly increasing failure rate (IFR). The Weibull Distribution allows us to model lifetimes having constant, strictly increasing, and strictly decreasing hazard functions. The Weibull Hazard Function, with parameters α and γ is given by:

$$h(t) = \alpha\gamma t^{\gamma-1} \quad \mathbf{t > 0} \quad \textbf{(9)}$$

where α and γ are positive constants. For $\gamma < 1$ we have a decreasing failure rate (DFR), for $\gamma > 1$ we have an increasing failure rate (IFR), and for $\gamma = 1$ we have a constant failure rate (CFR).

The cumulative Weibull Distribution F(t) is given by:

$$F(t) = 1 - \exp\left(-\int_0^t h(s)ds \right) = 1 - \exp\left(-\alpha t^{\gamma}\right) \quad \mathbf{t > 0} \quad \textbf{(10)}$$

The density function f(t) is given by:

$$f(t) = \alpha\gamma t^{\gamma-1} \exp\left(-\alpha t^{\gamma}\right) \qquad \mathbf{t > 0} \quad \textbf{(11)}$$

The survival function is given by:

$$S(t) = 1 - F(t) = \exp\left(-\alpha t^{\gamma}\right) \quad \textbf{(12)}$$

If a vector of explanatory variables $\underline{x}$ is observed with the duration data, the Weibull Hazard Function is given by:

$$h\left(t, \underline{x}, \underline{\beta}\right) = e^{-\gamma\mu}\gamma t^{\gamma-1} = e^{-\gamma \underline{x}^T \underline{\beta}}\gamma t^{\gamma-1} \quad \textbf{, t>0} \quad \textbf{(13)}$$

where $\mu = \underline{x}^T \underline{\beta}$**.** **(14)**

In this case the cumulative distribution function, the density function, and the survival function are respectively given by:

$$F\left(t, \underline{x}, \underline{\beta}\right) = 1 - \exp\left(-e^{-\gamma \underline{x}^T \underline{\beta}} t^{\gamma}\right) \quad \textbf{(15)}$$

$$f(t, \underline{x}, \underline{\beta}) = e^{-\gamma \underline{x}^T \underline{\beta}}\gamma t^{\gamma-1} \exp(-e^{-\gamma \underline{x}^T \underline{\beta}} t^{\gamma}) \quad \textbf{(16)}$$

$$S(t) = \exp\left(-e^{-\gamma \underline{x}^T \underline{\beta}} t^{\gamma}\right) \quad \textbf{(17)}$$

The parameters of the model, γ and $\underline{\beta}$, can be estimated by maximum likelihood. Meeker and Escobar (1998) give the expected time to cracking for a Weibull Model by:

$$E\left[t|\underline{x}\right] = e^{\mu}\Gamma\left(1 + \frac{1}{\gamma}\right) = e^{\underline{x}^T \underline{\beta}}\Gamma\left(1 + \frac{1}{\gamma}\right) \quad \textbf{(18)}$$

The gamma function, $\Gamma(z)$, is defined as:

$$\Gamma(z) = \int_0^{\infty} w^{z-1} e^{-w} dw \quad \text{for z > 0.} \quad \textbf{(19)}$$

2.4 The Cox Model

Parametric models like the Weibull Model have nice properties in that in most cases they allow closed form estimation of the survival and hazard functions. Moreover, they can be interpreted in a direct and simple manner, and are easier to use for prediction. Parametric models however impose more restrictions and structure on the survival and the hazard rate functions. Such restrictions might be inappropriate in certain cases when the data is more complex and appear to have a less structured distribution.

In these cases more general models that impose less structure on the survival and the hazard functions are more appropriate. The semiparametric family of models

allows this flexibility and the Cox model — also known as the "proportional hazard model" or the "relative risk model" — is one of the most flexible and widely used models of this type. The Cox model's analysis requires no assumptions regarding the form of the baseline hazard, and this is the main reason for the model's flexibility. For non-time variant covariates, the Cox hazard function is given by:

$$h(t) = h_0(t)\Psi(x) \quad \textbf{(20)}$$

where $h_0(t)$ is an arbitrary unspecified baseline hazard function that will be estimated, and

$$\Psi(x) = e^{\underline{x}^T \underline{\beta}} \quad \textbf{(21)}$$

where $\underline{x}$ is a vector of explanatory variables observed with the duration data and $\underline{\beta}$ is a vector of parameters that will be estimated by maximum likelihood.

The cumulative distribution function, the density function, and the survival function are respectively given by (Crowder et al 1991):

$$F(t) = 1 - [S_0(t)]^{\Psi(x)} \quad \textbf{(22)}$$

$$f(t) = f_0(t)\Psi(x)[S_0(t)]^{\Psi(x)-1} \quad \textbf{(23)}$$

$$S(t) = [S_0(t)]^{\Psi(x)} \quad \textbf{(24)}$$

where S_0 and f_0 are the baseline survival and density functions respectively, and are equal to S(t) and f(t) respectively when $\Psi(x) = 1, (\underline{x} = \underline{0})$

The baseline hazard function is:

$$h_0(t) = \frac{f_0(t)}{S_0(t)} \quad \textbf{(25)}$$

3.0 CRACK INITIATION MODEL OF ASPHALT CONCRETE OVERLAY

The PMS database provided by WSDOT (Washington State Department of Transportation) for use in this research included data for the years 1983 through 1999. The research team used the data to develop the crack initiation model of the AC (asphalt concrete) overlay. No new flexible pavements were included in the data set used for the model development. All observations used were of AC overlays of existing AC pavements.

3.1 Measurements and Characterization of Cracking

Alligator cracking and longitudinal cracking were the main types of overlay cracking of concern in this project. Below are the WSDOT definitions of each type of cracking and the agency's the measurement and recording methods (Kay et al 1992).

3.1.1 Alligator cracking

Definition:

Alligator cracking is associated with loads and is usually limited to areas of repeated traffic loading. Most load related cracking of this type begins as a single longitudinal, discontinuous crack within the wheel path that progresses with time and loads to a more branched pattern that begins to interconnect. The stage at which several discontinuous longitudinal cracks begin to interconnect is defined by WSDOT as alligator cracking. Eventually the cracks interconnect sufficiently to form many pieces, resembling the pattern of an alligator's hide.

Extent:

The extent of alligator cracking is related to the length of the wheel paths. A 100-foot segment has 200 feet of wheel path. WSDOT measures and records cracking as a percentage of wheel path length. The lengths along the surveyed lane of alligator cracking in both wheel paths are accumulated then divided by twice the length of the segment (two wheel paths per lane) then multiplied by 100 to get a percentage.

Example:

Segment length: 1/10 mile = 528 feet (1,056 feet of wheel paths).

Cracking in left wheel path	Cracking in right wheel path
125 ft	100 ft

Segment Total

225 ft (21%)

3.1.2 Longitudinal Cracking

Definition:

Longitudinal cracks run roughly parallel to the roadway centerline. Longitudinal cracks associated with the beginning of alligator cracking are generally discontinuous, broken, and occur in the wheel path. However, any longitudinal crack that is clearly within the traveled lane is rated even if outside the wheel path.

Extent:

The extent of longitudinal cracking is recorded as a percentage of the length of the surveyed segment. The lengths along the surveyed lane of longitudinal cracking are accumulated then divided by the length of the segment and multiplied by 100 to get a percentage.

Example:

Segment length: 1/10 mile = 528 feet

Recorded: 75 feet or 14%

Note: Since many longitudinal cracks might appear in parallel on the same lane, the recorded cracking according to the WSDOT method can exceed 100%.

In this project, we have set the threshold for overlay crack initiation at 5%. A pavement with 5% longitudinal or alligator cracking is considered to have cracked.

3.2 Washington PMS Data Description

The WSDOT has performed pavement condition surveys annually since 1983. The condition surveys covered most of the state highways. The surveys segmented the highways into 1/10-mile sections and measured variables such as pavement cracking and maintenance activity. This allowed the identification of different pavement types (concrete, asphalt, or composite) and the types of cracking (alligator, longitudinal, and transverse). Our research team also compiled traffic information and climate data for the different sections.

Following is a description of the relevant variables found in the Washington PMS database that were used in the model. The variables' names are those used in the model and are not necessarily WSDOT names.

- E_Long and E_Alli: Existing longitudinal cracking and alligator cracking, before rehabilitation. These variables represent the last measured cracking before the last rehabilitation activity was performed. They represent the distress level of the pavement before the overlay. These are important variables in modeling overlay cracking because overlay cracking is partly due to reflection cracking, which requires cracks in the previous pavement surface layer and their propagation through the overlay.
- Long and Alli: Overlay longitudinal cracking and alligator cracking. Each of these overlay cracks is reported on a yearly basis until the end of the experiment, which is defined by either the occurrence of further maintenance activity or the absence of more surveys.
- CUM_ESAL: Cumulative ESALs to initiation. CUM_ESAL is the sum of the ESAL from the year of the last overlay to the year when crack initiation occurs. If cracking does not occur by the end of the experiment then CUM_ESAL is the sum of the ESAL from the last overlay to the end of the experiment.
- SURFTHK: Layer thickness of the last overlay (in ft.)
- ULT: Sum of the thickness of the underlying asphalt concrete pavement layers (in ft.)
- Untrthick: the thickness of the non-treated base (in ft.)
- Actbthick: the thickness of asphalt concrete-treated base (in ft.)
- Pctbthick: the thickness of portland cement-treated base (in ft.)
- BA, AA: Dummy variables that take the value 1 if the material type of the overlay is "BA" or "AA," and 0 otherwise. The Washington PMS defines material types "BA" and "AA" as Asphalt Concrete Cements (ACP) that have the same binder type (AR4000W) and different mix classes. "BA," a class B mix, is described as a standard mix, with a maximum aggregate size of 5/8 in. "AA" is a Type A mix that also has a maximum aggregate size of 5/8 in., but

it uses a higher grade aggregate with more fractured rocks. A comparison of WSDOT and Caltrans specifications showed that the WSDOT Type A mix specification is very similar to the Caltrans specification for Type A dense-graded asphalt concrete; the largest aggregates in the gradation constitutes the primary difference between the two mixes. The WSDOT Type B mix falls in between the Caltrans Type A and Type B mixes: the WSDOT Type B mixes require more fractured faces than the Caltrans Type B mixes.

- Tmax: Average monthly maximum temperature of the hottest month (July, in ^{o}C) In hot climates, day and night temperature changes cause repeated thermal stresses in the surfacing that, in conjunction with stresses produced by traffic, contribute to reflection cracking.
- Tmin: Average monthly minimum temperature of the coldest month (December, in ^{o}C). Low temperatures contribute to cracking because cracks in the underlying asphalt open due to thermal contraction. This causes tensile strains in the overlay above the cracks. Moreover, cold temperatures make the AC overlay less viscous, which increases the rate of crack propagation because the unbound layers can not relax stresses.
- Prep: Annual precipitation (in mm). Precipitation and moisture in asphalt pavements can cause significant loss of strength of the underlying granular layers and the subgrade, thus weakening support for the asphalt concrete layers. In addition rainfall can also weaken the asphalt. All these factors will result in higher cracking.
- FTCycle: Annual number of Freeze-Thaw Cycles (number per year): Number of times that the air temperature trend crosses the freezing point, per year.
- FTprep: Product of FTCycle and Prep: Water that accumulates in the voids and cracks of the pavement freezes and increases in volume, creating more stresses and cracking. Water may also increase loss of cohesion in the asphalt mix. To reflect this in the model, the variable FTprep was created as the product of FTCycle and Prep.

- Prob_ba, Prob_aa, Prob_other: The probability of choosing material types BA, AA, or some other type, respectively. These variables are further explained in Section 3.3.
- Newoverlay1: Instrumented overlay thickness (in ft.). This variable is further explained in Section 3.3.

Table 1 shows the minimum, mean, and maximum values of each explanatory variable in the sample. The mean thickness of the overlay is relatively low (0.15 ft.), as are the mean values of the existing longitudinal and alligator cracking (29.4% and 4.98%, respectively). This suggests that WSDOT's overlaying strategy is to apply thin overlays on a frequent basis. The climate variables reflect the relatively cold (Tmin, -1.45°C; Tmax, 25.4°C) and rainy (Prep, 757 mm) weather of Washington State.

Table 1: The minimum, mean, and maximum of each explanatory variable in the sample

Variable	Minimum	Mean	Maximum
E_Alli (%)	0.00E+00	4.98E+00	8.00E+01
E_long (%)	0.00E+00	2.94E+01	2.55E+02
actbthick (ft.)	0.00E+00	3.90E-01	6.50E-01
pctbthick (ft.)	0.00E+00	5.00E-01	7.50E-01
untrthick (ft.)	0.00E+00	8.00E-01	2.83E+00
ULT (ft.)	6.00E-02	4.60E-01	1.90E+00
Tmax (°C)	1.40E+01	2.54E+01	3.80E+01
Tmin (°C)	-1.10E+01	-1.45E+00	4.00E+00
Prep (mm)	1.00E+02	7.57E+02	2.70E+03
Ftcycles (Numb.)	2.00E+00	8.60E+01	2.75E+02
SURFTHK (ft.)	3.00E-02	1.50E-01	6.00E-01

3.3 Model Specification

A Cox model was developed using approximately 7,000 observations (about one-third of the population data) from the Washington data source described earlier. Observations were chosen based on systematic sampling by picking the first observation from every set

of three observations. This sampling technique was used in order to reduce the risk of serial correlation in the data since the WSDOT database records are contiguous sections.

The dependent variable is the number of Cumulative ESALs to failure, where failure is defined as 5% alligator cracking or 5% longitudinal cracking, whichever occurs first. Several specifications that are linear in the parameters were tried using different combinations of the explanatory variables.

The function $\Psi(x) = e^{x^T \beta}$ that gives the best model is of the form

$$\Psi(x) = \text{Exp}\ (\beta_1 \text{E\_Alli} + \beta_2 \text{E\_Long} + \beta_3\ \text{actbthick} + \beta_4\ \text{pctbthick} + \beta_5\ \text{untrthick} + \beta_6 \text{ULT} + \beta_7 \text{Tmax} + \beta_8 \text{Tmin} + \beta_9 \text{FTprep} + \beta_{10} \text{Prob\_ba} + \beta_{11}\ \text{Prob\_aa} + \beta_{12}\ \text{newoverlay1}) \quad \textbf{(26)}$$

The variables E_Alli, E_Long, actbthick, pctbthick, untrthick, ULT, Tmax, Tmin, and FTprep are defined in Section 3.2. The variables newoverlay1, Prob_ba, and Prob_aa are the instrumented variables for SURFTHK, BA, and AA, respectively. In fact, the choice of the overlay thickness as well as the material type depends on the projected yearly ESALs, the previous conditions (existing cracking, etc.), and the previous structural strength. In order to correct for the endogeneity of the thickness of the AC overlay, the variable SURFTHK was regressed on projected yearly ESAL (1999 ESAL), structural variables (base thickness, thickness of previous AC layers), existing cracking, and climate variables. Based on this regression, a corrected or instrumented AC overlay thickness was created (newoverlay1) and later used in the Duration Model. In order to correct for the endogeneity of the material type, a multinomial logistic regression was performed on some of the same variables above as well as the instrumented AC overlay thickness (newoverlay1). This regression allowed the computation of the probability of choosing a certain material type (Prob_ba, Prob_aa, and Prob_other).

3.4 Model Results and Analysis

Our expectations of the effects of explanatory variables on the overlay life are as follows: we expect that better structural conditions increase the overlay life. Accordingly an increase in the thickness of the overlay, an increase of the untreated or treated base, and an increase in the thickness of underlying asphalt concrete layers, would increase the overlay life (Cumulative ESALs to failure) by increasing the strength of the pavement. An increase in the existing cracking before rehabilitation is expected to decrease the life of the overlay. If existing cracking before rehabilitation is a significant explanatory variable, this would support our hypothesis that overlay cracking is at least partly due to reflection cracking. We would also expect that as the minimum temperature increases, the occurrence of low temperature cracking in the asphalt overlay decreases, which increases the life of the overlay. Precipitation is expected to decrease the life of the overlay and to

accelerate cracking because water infiltrates to the granular layers and the subgrade, and makes them softer, which weakens support for the asphalt layers and renders them more susceptible to cracking. Moreover precipitation can weaken the asphalt overlay. freeze-thaw cycles, in the presence of water from precipitation, also tend to decrease the life of the overlay because they lead to an increase in volume, which widens existing cracks. Higher maximum temperatures were expected to soften the asphalt, reducing the support of underlying asphalt layers, increasing the strains in the overlays, and shortening lives.

Table 2 shows the results of the estimation of the parameters of Equation (26). These results confirmed our expectations of the correctness of the signs. Furthermore, the t-statistics show that each variable is a significant explanatory variable of crack initiation at the five percent significance level. Moreover, we learn from the models that the AA material type is better than the BA material type, but that both are worse than the average material type in the sample. In addition, treated base appears to be significantly better (by one order of magnitude) in extending the life of the overlay than the non-treated base, and asphalt-treated base appears to be slightly better than portland cement-treated base.

In order to test the prediction power of the Cox model, the estimated survival and hazard functions (Figures 7 and 8, respectively) were plotted and compared to the nonparametric estimates of the survival and hazard functions plotted using the sample data (Figures 5 and 6, respectively). It is clear comparing Figure 7 to Figure 5, and Figure 8 to Figure 6, that the new model has good predictive power. *(Note:* The model estimations and predictions were made using the *Stata 8* software and manuals developed by the Stata Corporation, 2003.)

Table 2: Cox Model Coefficients Estimates. *(Note*: Positive coefficients indicate negative effect on the the cumulative ESALs to 5% cracking)

Variable	Coefficient	t-statistic
E_Alli	2.79E-02	1.38E+01
E_long	6.40E-03	1.13E+02
actbthick	-2.44E+00	-1.17E+01
pctbthick	-7.91E-01	-8.57E+00
untrthick	-5.37E-01	-1.33E+01
ULT	-5.50E-01	-7.99E+00
Tmax	-5.63E-02	-1.21E+01
Tmin	-1.88E-01	-2.43E+01
Ftprep	6.62E-05	2.01E+01
newoverlay1	-3.31E+01	-1.08E+01
Prob_aa	8.73E+00	1.33E+01
Prob_ba	1.11E+01	1.64E+01

Number of observations	7132

The survival function estimates indicate that around 15% of the sections survive past 500,000 cumulative ESALs, and that less than 5% survive past 1,000,000 cumulative ESALs. Figures 6 and 8 show a hazard rate that decreases initially for cumulative ESALs less than 500,000 then starts an increasing trend past this value. The hazard rate shoots high after reaching 1,000,000 cumulative ESALs. This hazard rate trend suggests that weak overlays fail early, and that overlays that live long enough have a lower probability of failure until they reach a certain point. After that point they deteriorate rapidly, which leads to a rapid increase of their probability of failure. This hazard rate shape is often

observed in natural phenomena (e.g., the hazard function depicting human life with a high infant mortality that is followed by a low death rate, which in turn followed by a death-rate increase due to old age) and is referred to as a "bathtub hazard function." Another explanation for this hazard function's behavior is this: sections that live long enough receive routine maintenance that further extends their life and reduces their hazard rate. When these sections pass a certain life (500,000 cumulative ESALs) they start deteriorating rapidly and routine maintenance becomes ineffective. Neither of these explanations has been investigated.

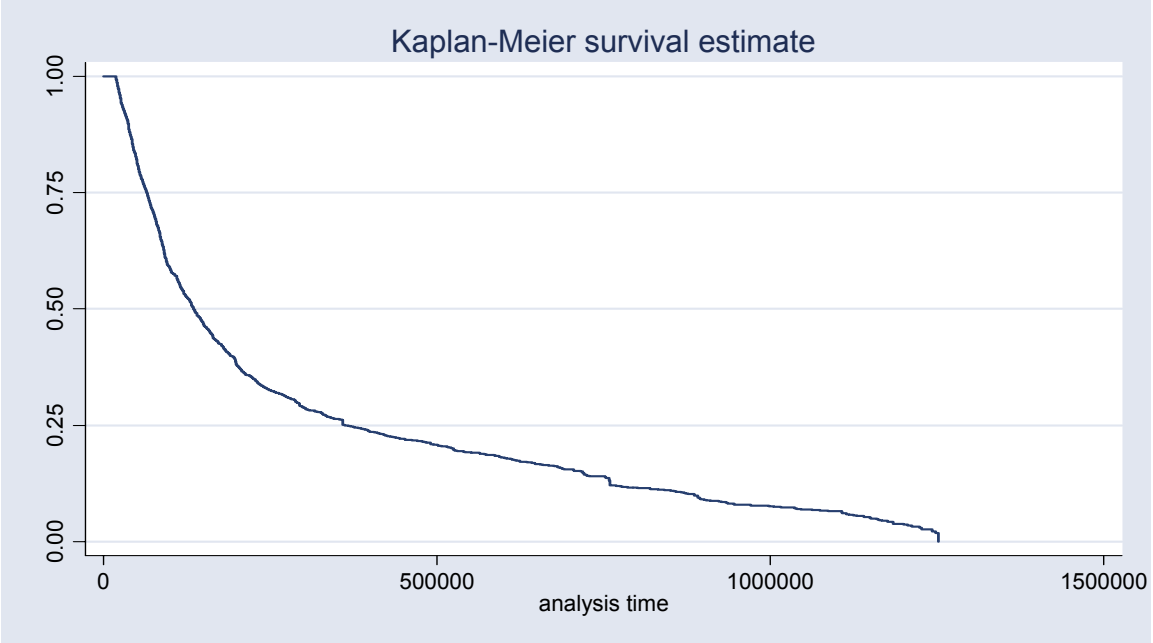

Figure 5: Non-parametric plot of the survival function

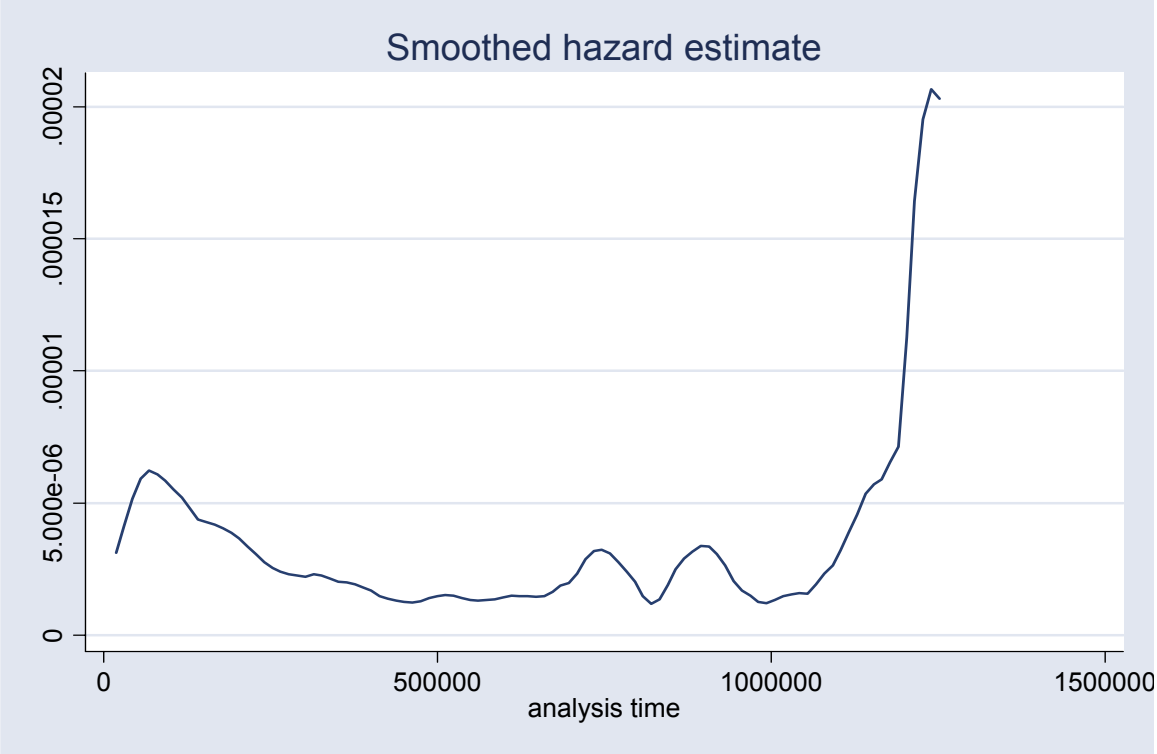

Figure 6: Non-parametric plot of the hazard function

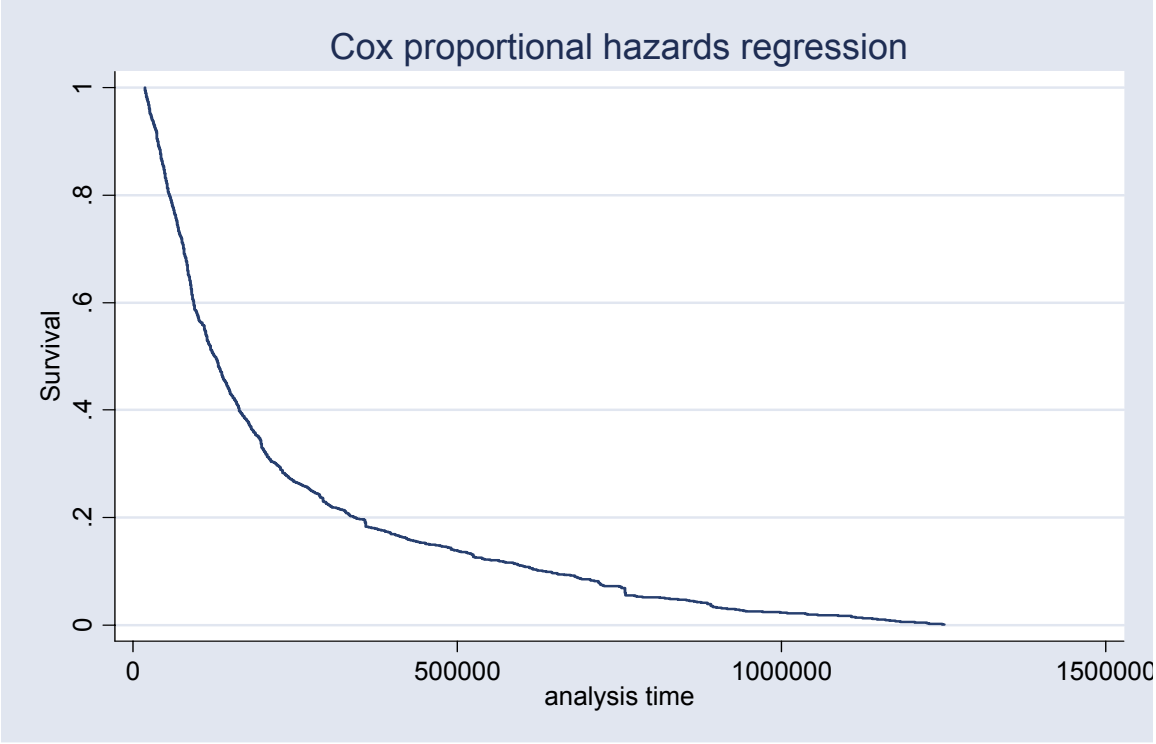

Figure 7: Model prediction of the survival function

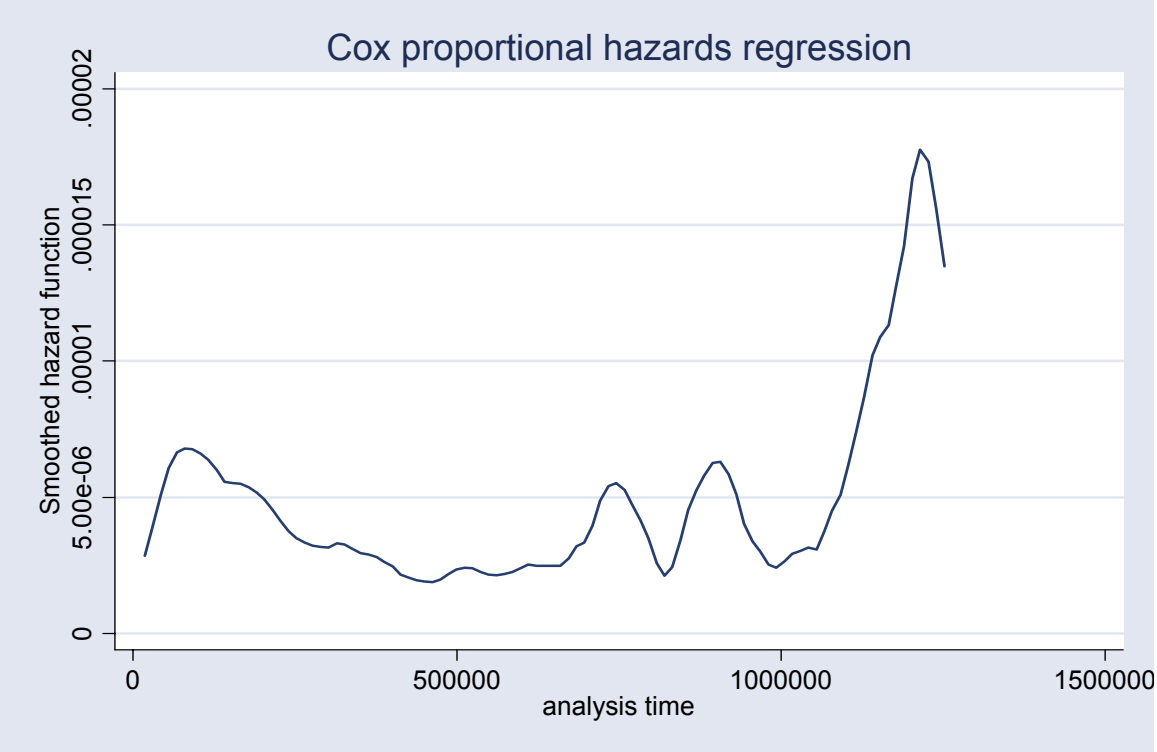

Figure 8: Model prediction of the hazard function

3.5 Model Predictions and Sensitivity

In this section we will perform a parametric study to illustrate the importance of performance models on infrastructure maintenance policies.

We compute the expected ESALs to 5% cracking for each variable at its Mean sample value, at the mean +/- one standard deviation (S), and at mean +/- 3S (Table 3), while keeping all other explanatory variables fixed at their mean values. For all the graphs produced, we also varied the overlay material type (AA, and BA). It should be noted that for some variables, the Mean-S, or Mean-3S fell outside a meaningful range (such as a negative value for the overlay thickness) and were omitted from the graphs.

The results presented in Figure 9 show that an overlay's thickness has the largest effect on its life. The overlay material type is another important variable; choosing a different material type can more than triple the life of an overlay. The thickness of the underlying layers (Figure 10) and the thickness and type of the base also appear to be important (Figures 11, 12, and 13). These findings are particularly important since surface thickness, material type, and thickness of the underlying layers are among the

main variables considered in maintenance policies. The decrease of the overlay life with an increasing percentage of existing alligator and longitudinal cracking (Figures 14 and 15) confirms the hypothesis that overlay cracking is at least partly due to reflection cracking. Consideration of climate variables, such as the average minimum temperature of the coldest month (Figure 16), the average maximum temperature of the hottest month (Figure 17), and the product of freeze-thaw cycles and annual precipitation (Figure 18), is also important in determining the life of the overlay, but less so than that of the main structure variables. Figures 19 through 21 compare the relative effect of each explanatory variable on the life of the overlay. . However, it should be noted that the Mean-S, the Mean, and the Mean+S values differ for each explanatory variable, and this should be considered when making comparisons.

Table 3: The Mean, Mean +/-S, and Mean +/- 3Ss of Each Explanatory Variable in the Sample

Variable	Mean-3S	Mean-S	Mean	Mean+S	Mean+3S
E_Alli	N/A	N/A	4.98	12.33	27.02
E_long	N/A	5.58	29.39	53.19	100.81
actbthick	0.05	0.28	0.39	0.50	0.72
pctbthick	0.42	0.47	0.50	0.52	0.57
untrthick	-0.40	0.40	0.80	1.20	2.00
ULT	-0.19	0.24	0.46	0.67	1.10
Tmax	14.55	21.81	25.44	29.08	36.34
Tmin	-11.29	-4.73	-1.45	1.83	8.39
Ftprep	N/A	N/A	22,192.30	45,277.68	91,448.44
newoverlay1	N/A	0.09	0.15	0.21	0.33

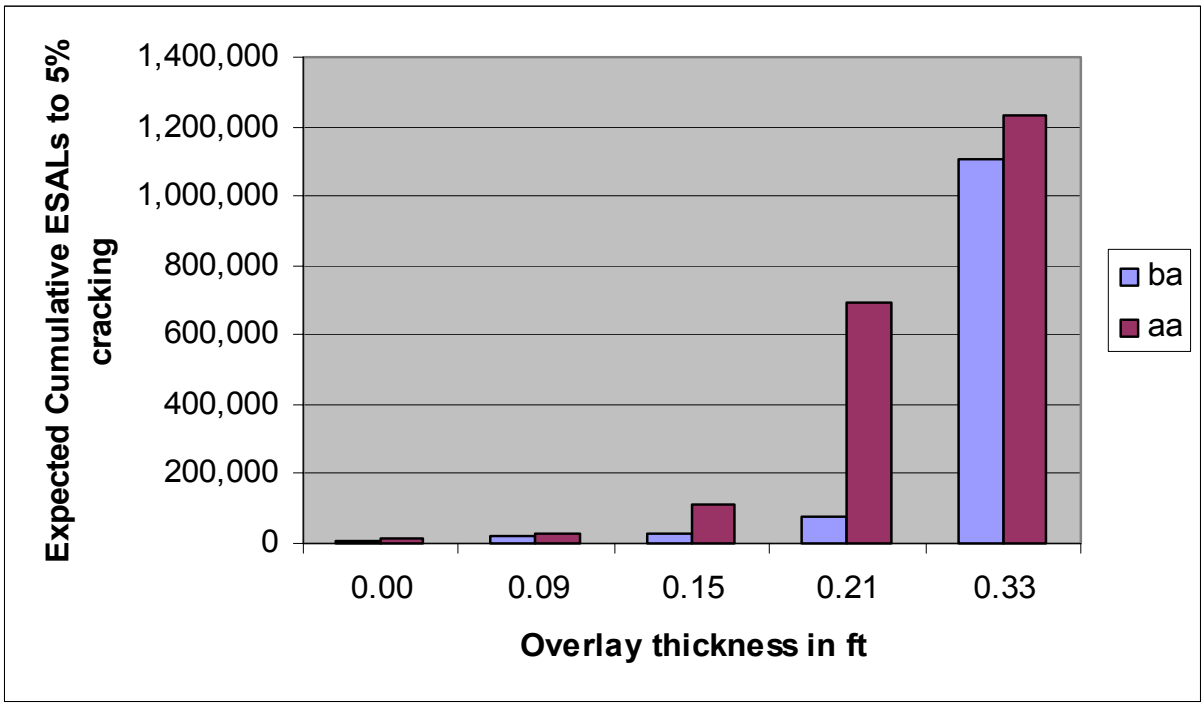

Figure 9: The effect of AC overlay thickness on overlay life

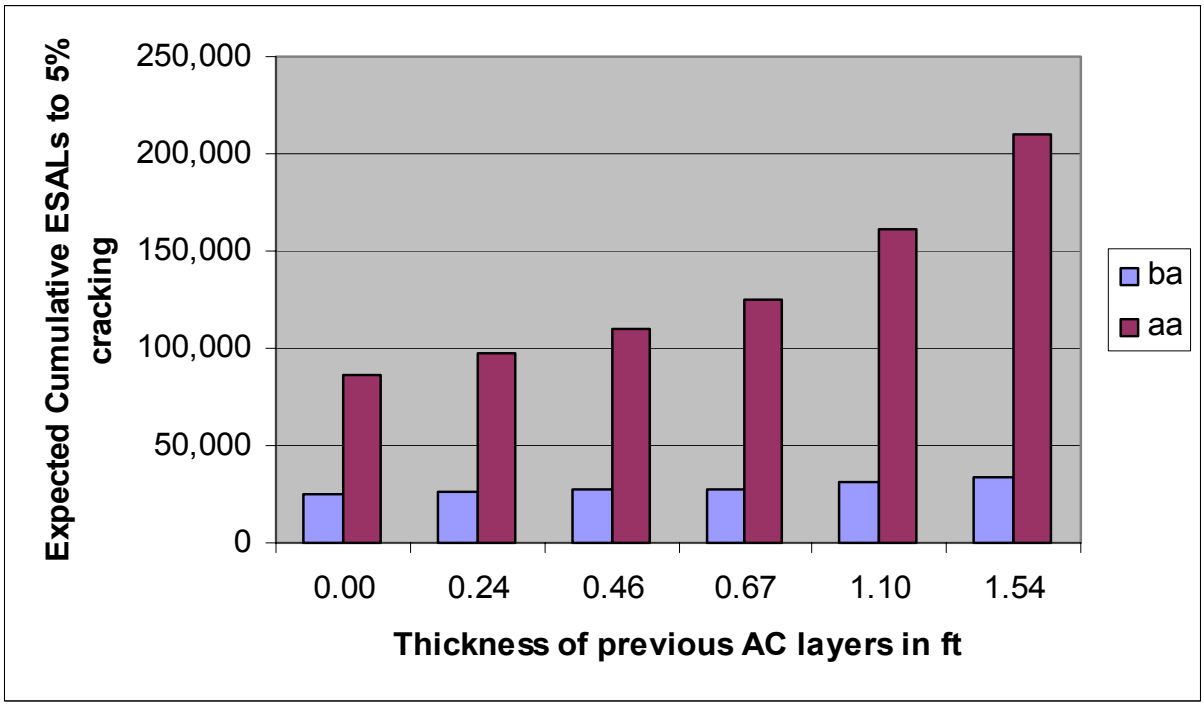

Figure 10: The effect of the thickness of previous AC layers on overlay life

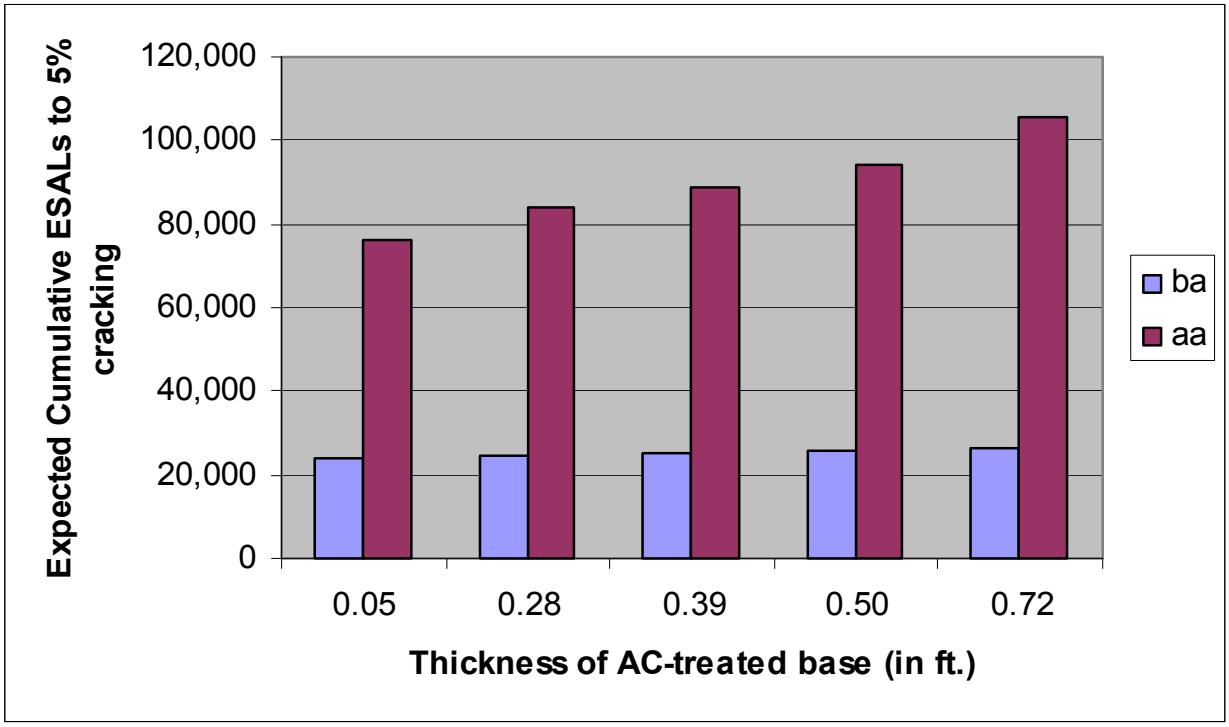

Figure 11: The effect of the thickness of AC-treated base on overlay life

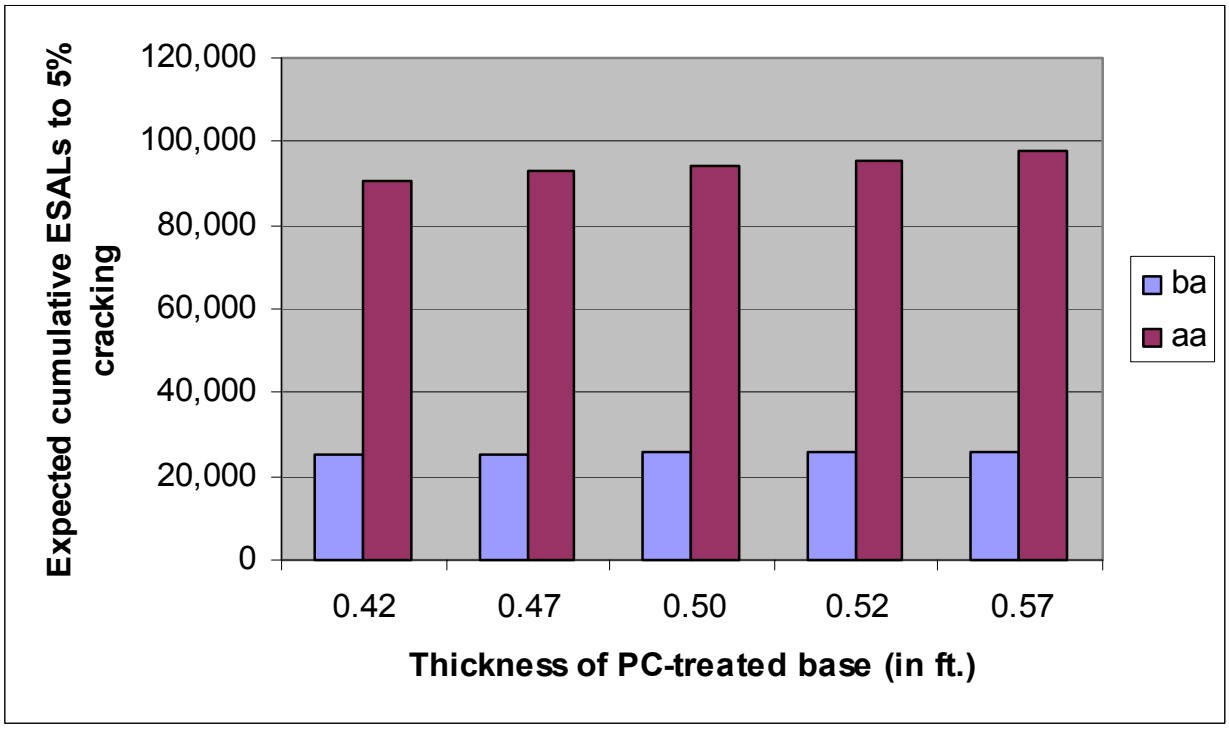

Figure 12: The effect of the thickness of PC treated base on overlay life

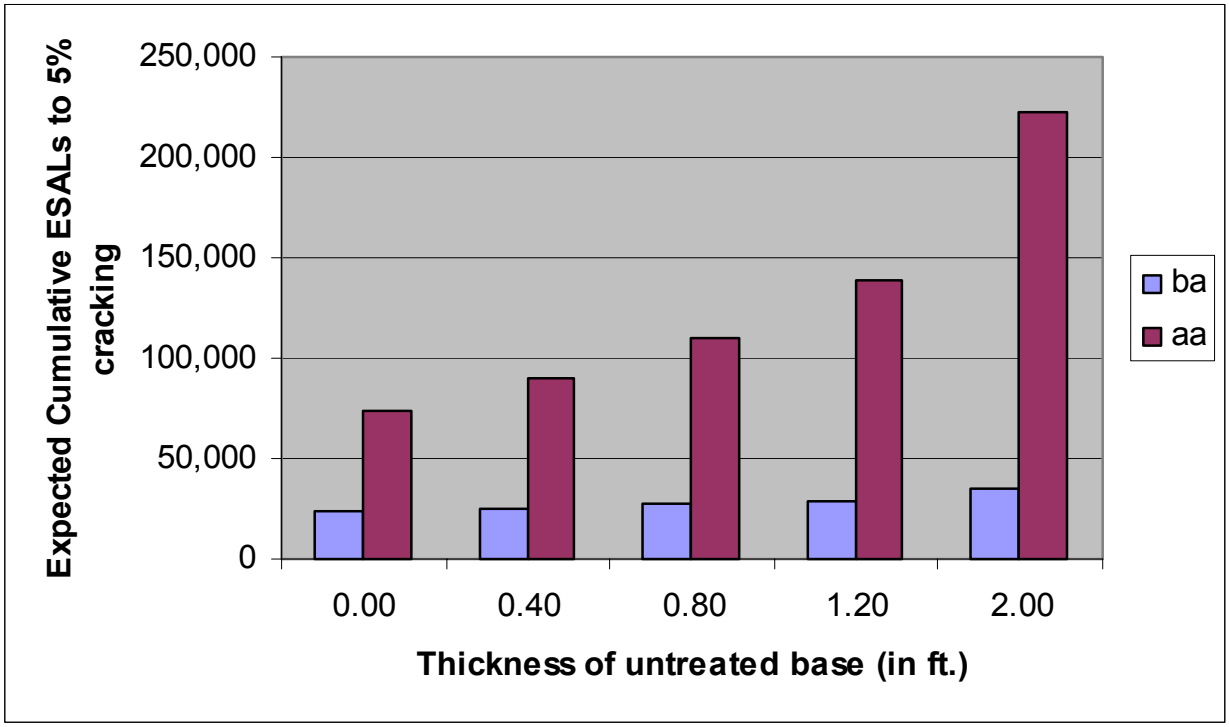

Figure 13: The effect of the thickness of untreated base on overlay life

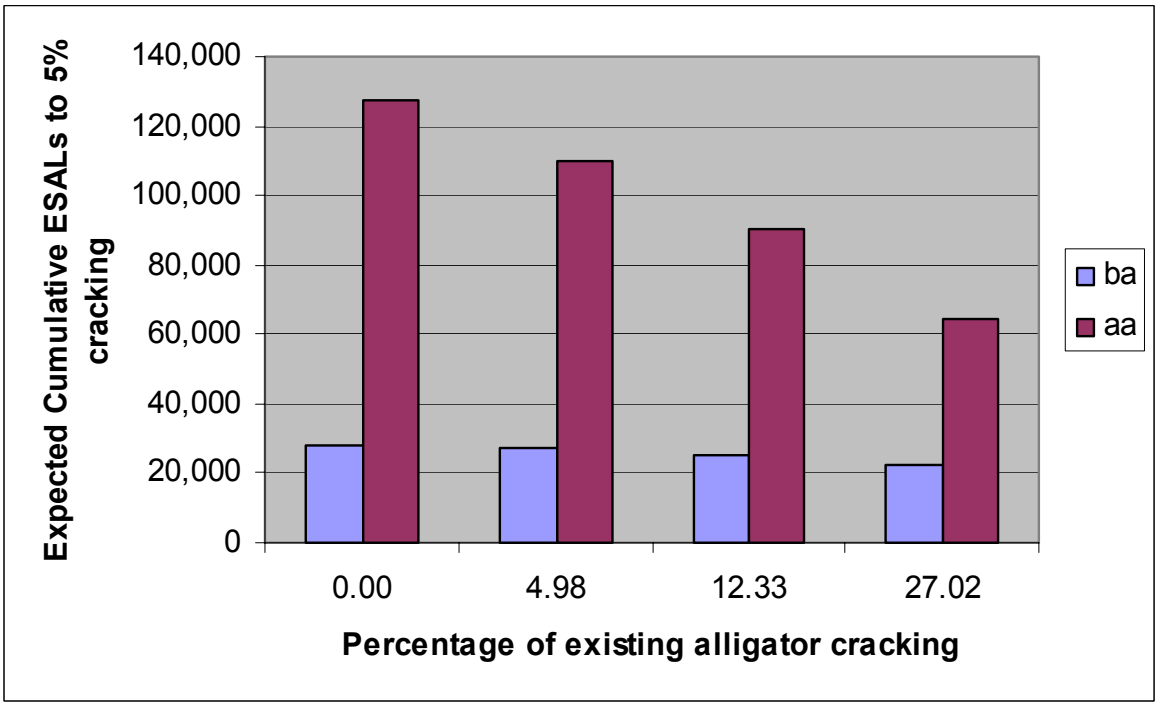

Figure 14: The effect of the percentage of existing alligator cracking on overlay life

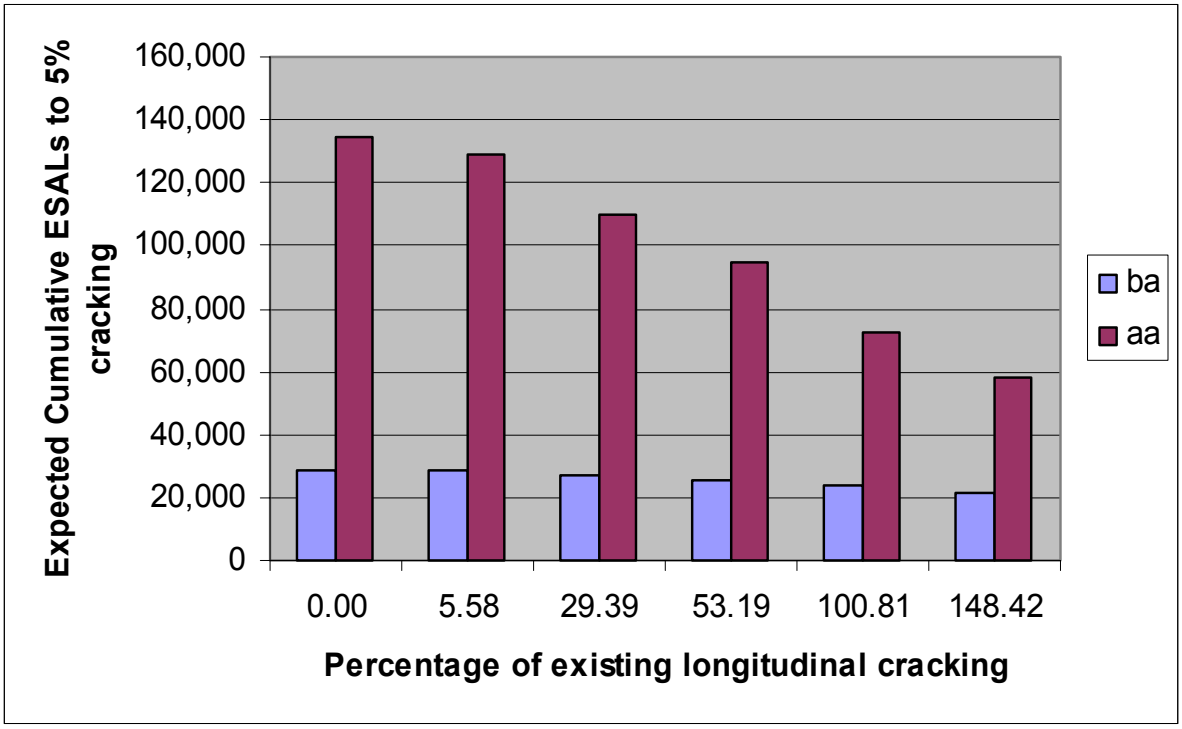

Figure 15: The effect of the percentage of existing longitudinal cracking on overlay life

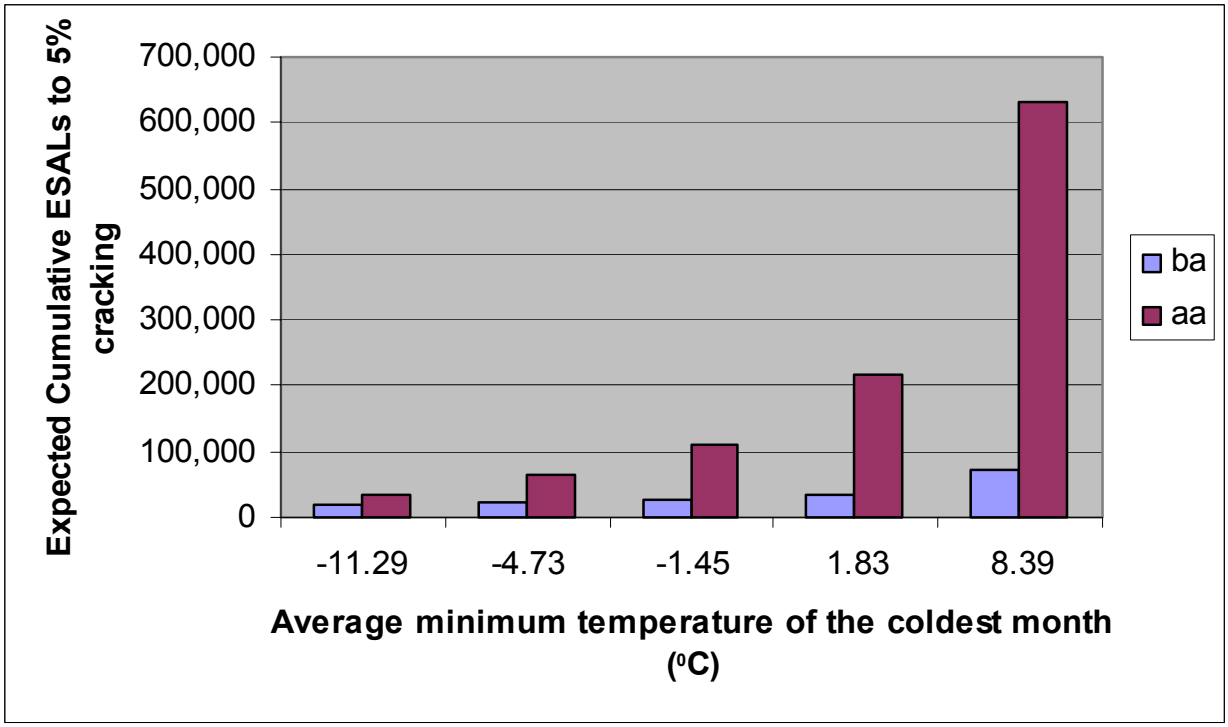

Figure 16: The effect of the average minimum temperature of the coldest month on overlay life

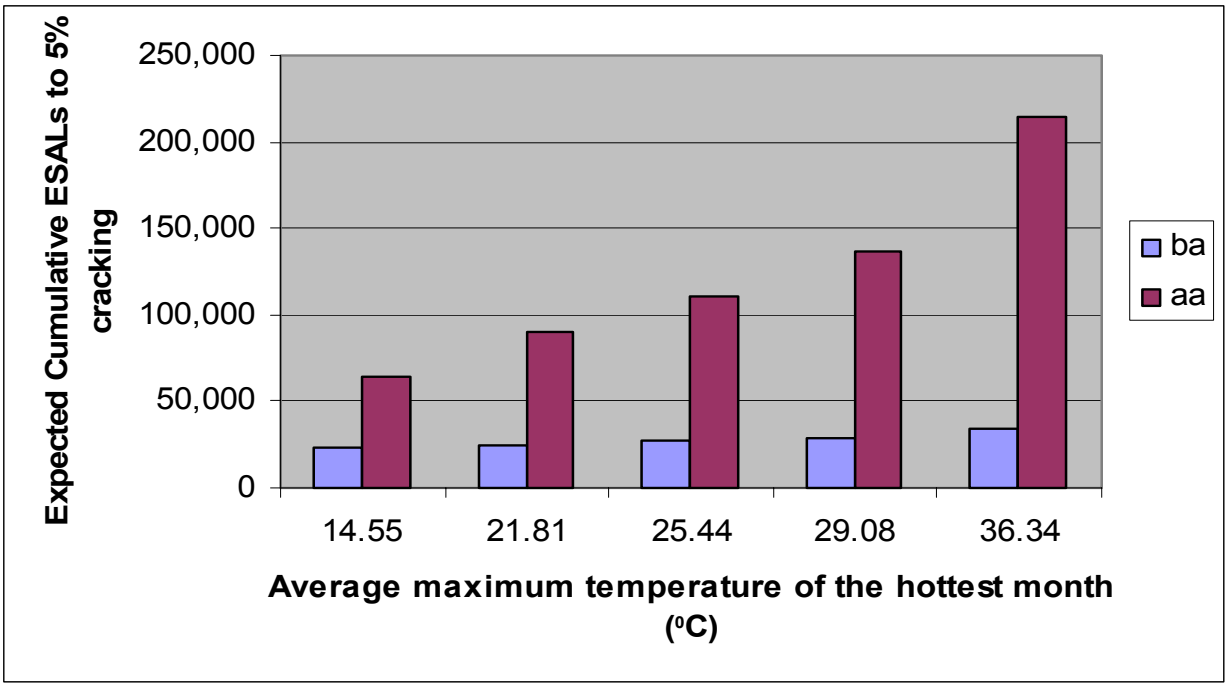

Figure 17: The effect of the average maximum temperature of the hottest month on overlay life

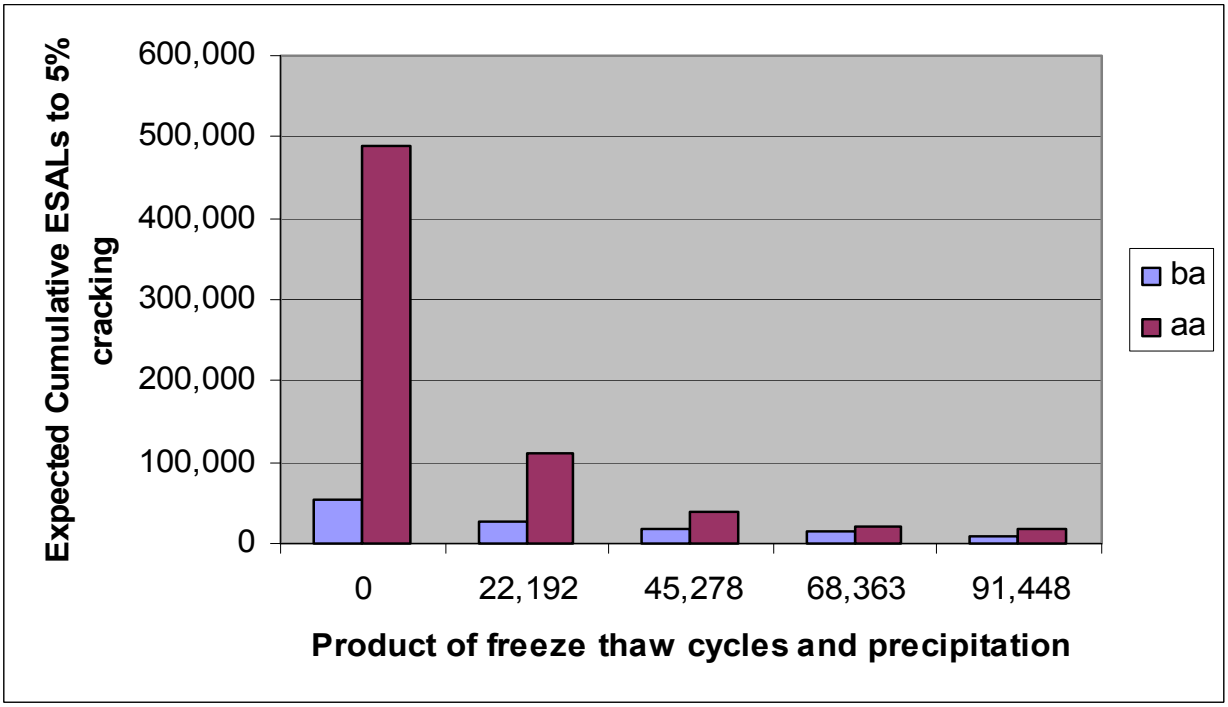

Figure 18: The effect of the product of freeze-thaw cycles and precipitation on overlay life

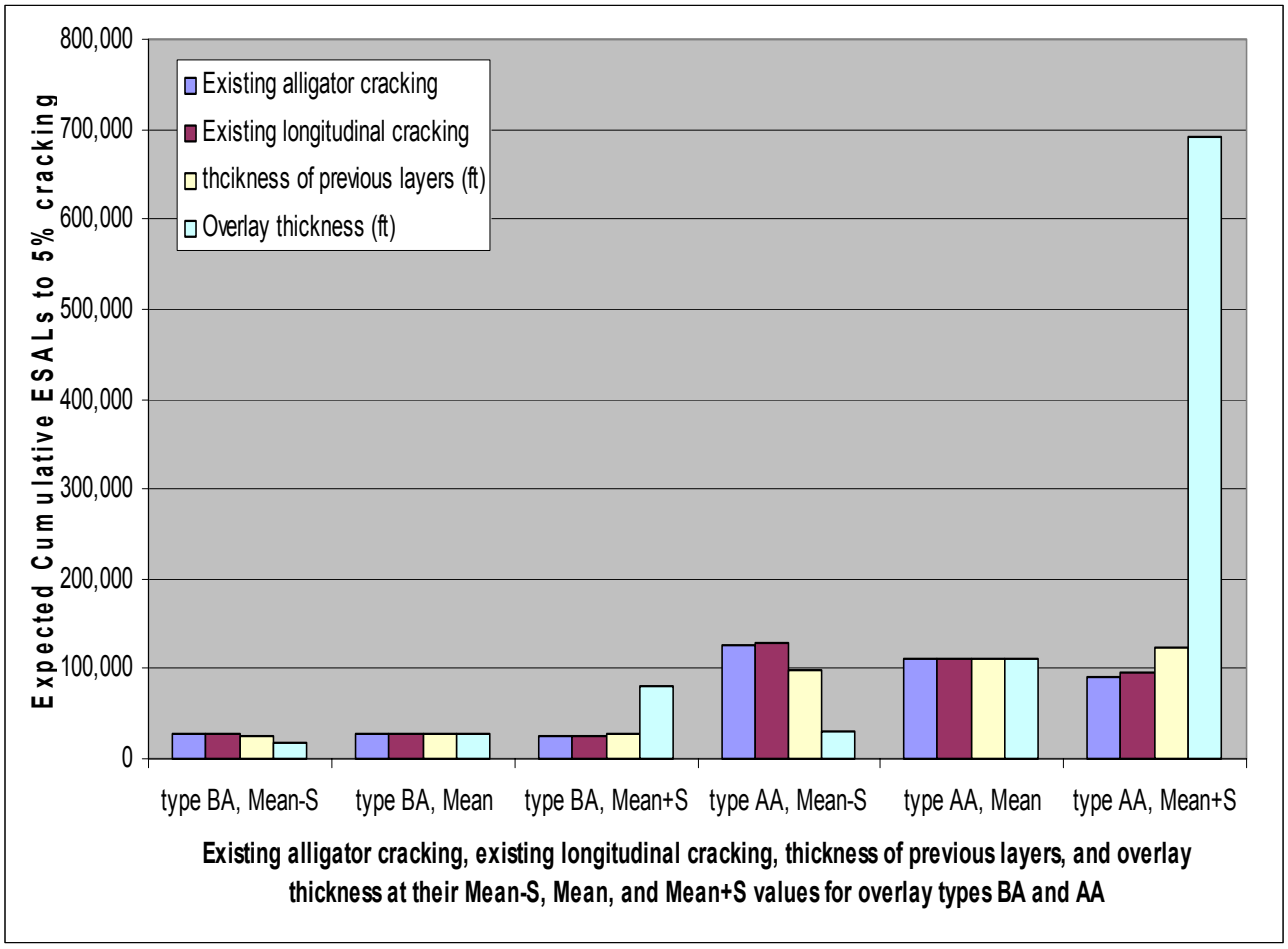

Figure 19: Comparison of the effect of existing alligator cracking, existing longitudinal cracking, thickness of previous layers, and overlay thickness on life of the overlay

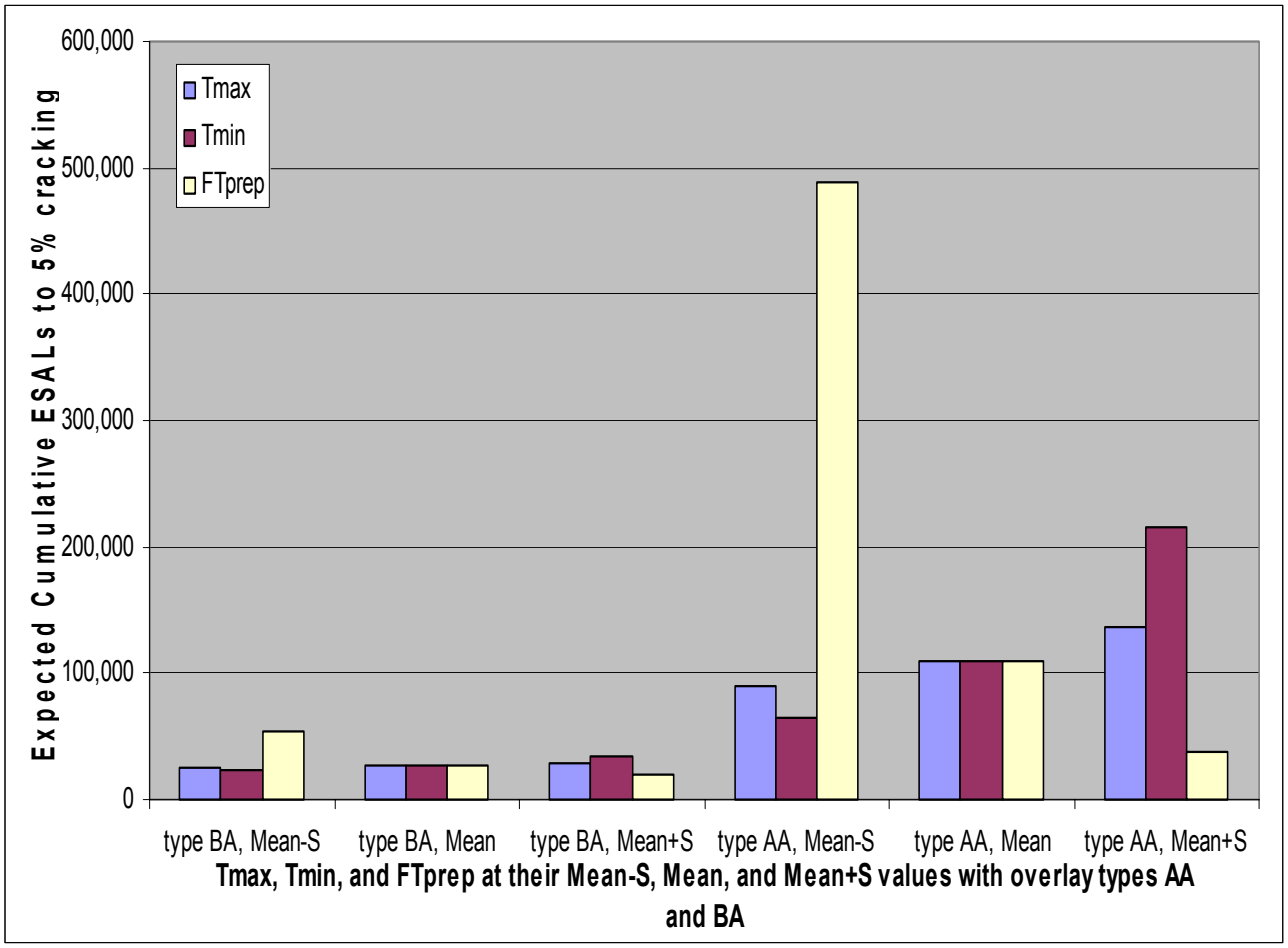

Figure 20: Comparison of the effect of the average maximum temperature of the hottest month, the average minimum temperature of the coldest month, and the product of precipitation and freeze-thaw cycles on the life of the overlay

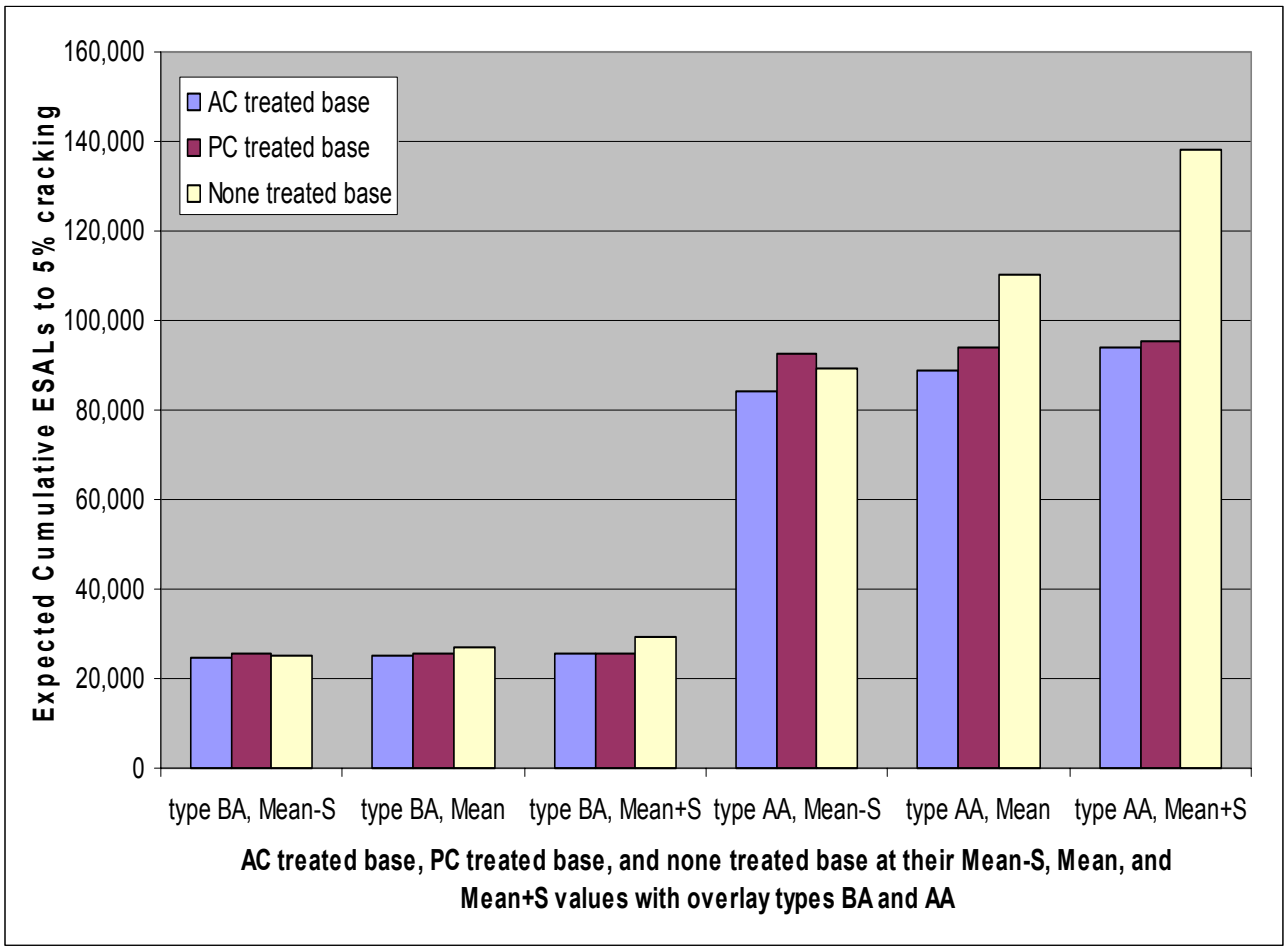

Figure 21: Comparison of the effect of the AC-treated base, PC-treated base, and none treated base on the life of the overlay

4.0 ASPHALT CONCRETE ROUGHNESS PROGRESSION MODEL

4.1 Review of Linear Regression

Linear regression is used to develop a model that predicts incremental roughness progression based on the Washington State Pavement Management System (WSPMS) database. Initially, Ordinary Least Squares (OLS) regression is employed to find a model that is both statistically significant and valid in the sense that the explanatory variables are causally linked to roughness progression. Once a reasonable model is obtained using OLS, a second one is estimated using the Random Effects Model approach to account for unobserved heterogeneity.

OLS regression is performed to estimate a linear model that helps explain the effects on a dependent variable resulting from shifts in specified explanatory variables. Equation 27 exhibits the general form of the linear regression model where y represents the dependent variable and x_K is the explanatory variable value with an estimated coefficient of β_K for each variable denoted by the value of subscript K. β_0 is the estimated constant, ε is the random error term, and the subscript i denotes each observation in the dataset.

$$y_i = \beta_0 + \beta_1 x_{i1} + \beta_2 x_{i2} + \ldots + \beta_K x_{iK} + \varepsilon_i \quad \textbf{(27)}$$

The following assumptions are made when employing OLS (Pindyck and Rubinfeld 1981).

- Equation 27 gives the model specification.
- The x's are nonstochastic. In addition, no exact linear relationship exists between two or more of the independent variables.
- The error term has 0 expected value and constant variance for all observations.
- Errors corresponding to different observations are uncorrelated.
- The error variable is normally distributed.

The coefficients of the linear model are estimated by minimizing the sum of the squared deviations of the observed dependent variable values from the fitted line. This concept is restated formally in Equation 28, where i denotes each observation, Y_i is the

observed value of *Y*, the dependent variable, and $\hat{Y}_i$ is the estimated value of *Y* that lies on the fitted line.

$$\text{Minimize} \sum (Y_i - \hat{Y}_i)^2 \quad \textbf{(28)}$$

The use of matrix notation provides a concise solution to the estimation of coefficients based on the objective described by Equation 28. Equation 29 shows the solution, where $\hat{\beta}$ = k*1, a dimensioned column vector of estimated coefficients including the constant, $\underline{Y}$ = N*1 column vector of dependent variable observations, and $\underline{X}$ = N*k matrix of explanatory variable observations. N is the number of observations in the dataset, and k is the number of explanatory variables including the constant which takes on the value 1 for all observations. The derivation of this result involves the use of calculus and can be found in standard econometrics literature (Pindyck and Rubinfeld 1981).

$$\hat{\beta} = (\underline{X}'\underline{X})^{-1}(\underline{X}'\underline{Y}) \quad \textbf{(29)}$$

After finding a valid model through OLS, further refinement can be made by accounting for the fact that the observations take the form of a panel dataset. This refinement requires considering each observation to be a measurement of the characteristics of a length of pavement section at a particular point in time (which is why it comprises a panel dataset.) Further calibration is necessary because panel datasets often have some unobserved heterogeneity, or cross-sectional variation, which persists through time. Therefore, a second error term is added that captures this variation; this approach is known as a Random Effects Model. It accounts for the panel dataset by including error terms for both observations and sections. Equation 30 shows the form of the model equation; in it the coefficients and explanatory variables described for Equation 28 reappear.

$$y_{jt} = \beta_0 + \beta_1 x_{jt1} + \beta_2 x_{jt2} + \ldots + \beta_K x_{jtK} + \varepsilon_{jt} + \nu_j \quad \textbf{(30)}$$

The aforementioned assumptions for OLS apply to the Random Effects Model as well, except that Equation 30 now gives the model specification, the variance for the error term across observations is not assumed to be constant, and the errors for different observations may be correlated. The two error terms are also assumed to be uncorrelated

with one another, errors for different sections are assumed to be uncorrelated, and the expected value for the new error term is equal to 0.

For the Random Effects model, a two-step Generalized Least-Squares (GLS) is applied. GLS can be applied to cases in which serial correlation and heteroscedasticity are present. In the first step, the variance components are estimated by using the residuals from OLS regression. In the second step, feasible GLS estimates are computed using the estimated variances. Equation 31 presents the resulting formula used to estimate the coefficients using the Random Effects approach. The matrices used to estimate the slopes for OLS are again used for the Random Effects Model. In addition, $\underline{V}$ represents a consistently estimated N*N-dimensioned matrix of correlation coefficients for the error term values. The derivation of this result can be found in standard econometrics literature (Greene 1993).

$$\hat{\beta} = (\underline{X}'\underline{V}^{-1}\underline{X})^{-1}(\underline{X}'\underline{V}^{-1}\underline{Y}) \quad \textbf{(31)}$$

4.2 Dataset

The WSPMS database uses the value International Roughness Index (IRI) to represent the extent of roughness on pavement sections. IRI, which is measured in the dimensionless unit cm/km, represents the results of simulation of a quarter of a passenger car responding to the vertical deviations in a pavement surface per length of roadway in terms of the vertical movement of the car body and therefore the passenger. This model uses the change in IRI (ΔIRI) divided by the number of years between observations as its dependent variable.

The model also contains eleven explanatory variables, which are listed in Table 4 with their estimated coefficients and t-statistics. The first variable is the previous year's IRI because it indicates how great the rate of IRI progression is affected by the extent of previously recorded roughness. Accordingly, the previous IRI variable contributes to indicating the curvature for the IRI curve as a function of time.

The length of time that has passed since the last AC or bituminous surface treatment (BST) overlay also affects the curvature of the IRI function because it provides a representation of how long has passed since the last major repair activity.

The final variable affecting the curvature is the cumulative ESALs variable, which accounts for the effect of total traffic loading since the most recent AC overlay.

Recognizing that many of the valid observations in the dataset actually exhibit a decrease in IRI, three independent variables have been incorporated into the model to capture the effects of maintenance and rehabilitation. The maintenance dummy is set equal to 1 for observations that do not occur during a recorded AC or BST overlay year, but do have a negative ΔIRI. On the other hand the AC overlay dummy is set equal to 1 for observations made during an AC overlay year and exhibit a negative ΔIRI; the BST dummy is set equal to one in the case of a BST overlay year and a negative ΔIRI. Observations that have a positive ΔIRI are assigned values of 0 for all three dummy variables.

These variables allow four different intercept parameters to be computed for the cases of maintenance, AC overlay, BST overlay, and deterioration only. The intercepts are calculated by the addition of the estimated constant and the appropriate dummy coefficient in the case of repair, and only by the constant in the case of no repair.

Two variables are included to represent the strength of the pavement structure. The first variable is the total thickness of the asphalt surface layers, which is directly impacted by traffic and is also the layer on which roughness is measured. The base thickness is included to represent the strength of the underlying layers. The base layer provides support for the surface layers.

The model also captures the effects of yearly traffic and the environment through three variables. The ΔESALs variable provides a representation of traffic loading, which has impacted the pavement during the observation year, because heavy traffic can significantly increase the deterioration rate. Two final variables incorporated capture the effects of the environment on pavement deterioration. Because water can significantly damage pavements; an annual precipitation variable has been included. Finally, the model includes a variable for minimum yearly air temperature because low temperatures can severely weaken pavements by causing them to become very brittle.

Certain observations are omitted from the dataset. These include observations for in which valid measurements are not available for the explanatory or dependent variables. They are also omitted because the concept of pavement management had not begun

implementation until around 1980. Accordingly, observations made of pavement sections where overlay was applied before 1980 have been removed because it is assumed that measurements at that time were inaccurate. After these data were removed, only half of the pavement sections were used to estimate the model. The predictive capability of the model was tested on the remaining sections.

4.3 Estimation Results

Table 4 displays the estimated Random Effects Model for roughness progression.

Table 4: Estimated Roughness Progression Model

Explanatory Variable	**Coefficient**	**t-statistic**
Constant	52.0918	89.276
IRI in previous year (cm/km)	-0.171	-111.615
ΔESALs in year of observation (millions of ESALs)	3.371	2.949
Cumulative ESALs (millions of ESALs)	-1.713	-10.075
Base Thickness (ft.)	-1.868	-8.166
Total Thickness of AC Overlays (ft.)	-5.661	-15.151
Time since last AC or BST overlay (yrs.)	0.826	24.668
AC Overlay Dummy	-64.196	-120.851
BST Overlay Dummy	-50.512	-25.323
Maintenance Dummy	-50.603	-262.981
Minimum Air Temperature (°C)	-0.174	-10.066
Yearly Precipitation (in.)	0.026	5.963
Number of Observations = 109,107	**Number of Sections = 16,659**	
R-squared = .526	**Dependent Variable: ΔIRI (cm/km)**	

The magnitude of the error terms indicates that the variation across sections does not have a large effect relative to the variation across observations, since ε_{jt} is an order of

magnitude greater than ν_j The t-statistics indicate that all coefficients have a level of significance greater than 99.5%, since the lowest is 2.949. This shows that all the explanatory variables along with their coefficients have significant effects on roughness progression. Also, the R-squared value is reasonably high considering that the model is predicted using field data. The value indicates that 52.6% of the total variation in the dependent variable is explained by the model.

The signs for the coefficients are generally as expected with the layer thicknesses, minimum air temperature, and dummies having negative signs, indicating that thicker pavements, higher minimum air temperatures, and repair activities reduce roughness progression. In addition, the positive signs on the yearly traffic loading and precipitation coefficients correspond with the increase in ΔIRI caused by these variables. The sign for the time since the last overlay indicates that the rate of roughness progression increases with age; however, the signs of the previous IRI and cumulative ESALs coefficients are negative, suggesting that ΔIRI decreases with increases in the previously recorded IRI and total traffic loading, contrary to expectation. This is a somewhat counterintuitive result; however, the data has some measurement error and certain assumptions have been made in its structuring. For instance the many negative values for the ΔIRI found in the dataset are a significant concern, since the roughness should be generally increasing. In addition, the overlay years do not necessarily match the significant decreases in IRI, and information regarding the timing of surveys in relation to those for overlays is not provided. These problems may also be exhibited in the magnitudes of the dummy coefficients, since the maintenance dummy coefficient is nearly equal to the BST dummy coefficient and the two are fairly close to the magnitude of the AC dummy coefficient. One would expect a contrary result with the AC dummy coefficient far more negative than the other two, and the BST dummy more negative than the maintenance dummy.

4.4 Prediction Results

Figures 22 through 24 display the observed versus predicted ΔIRI on different axes scales. The predicted ΔIRI values are calculated using the estimated roughness model on the second half of the pavement sections, which were separated prior to model estimation. As can be inferred from Figure 23, the model generally does not tend to

underestimate or overestimate the ΔIRI when the observed value is between about -70 to -15 cm/km, and between 5 to 40 cm/km, since the data spreads evenly above and below the 45-degree line. This line represents cases in which the predicted value equals the observed value. For observed values of ΔIRI between about -15 and 5 cm/km, the model does tend to overestimate the magnitude of ΔIRI as can be seen in Figure 24. In this range, many of the data points lie above the line for observed ΔIRI values greater then 0, and for observed values below 0, the predicted ΔIRI often lies below the line. On the other hand, for cases in which the observed ΔIRI has a high magnitude, above 40 cm/km or below -70 cm/km, the model tends to underestimate the dependent variable. To some extent, this result can be expected because of the presence of outliers. Figure 25 indicates that over 85% of the observations have observed ΔIRI values between -70 cm/km and 40 cm/km. Therefore, only a small percentage of the observations have been underestimated. On the other hand a larger percentage – about 30% – of the observed ΔIRI values is close to 0, in which case the magnitudes are sometimes overestimated.

Figures 26 through 30 display deterioration predictions for roughness progression based on the mean values for the half of the dataset on which the model has been estimated. Also, the ΔESALs, base thickness, asphalt surface thickness, minimum temperature, and yearly precipitation values are varied by one and two standard deviations from the Mean, producing multiple curves in the figures. This provides an indication of the shift in roughness progression resulting from variation in the explanatory variable values. As displayed in Figure 28, variations in the asphalt surface layer thickness value causes significant shifts in the resulting IRI curve. Variations in base thickness, minimum temperature, and yearly temperature cause some shift in the IRI curve and nearly no change occurs due to variations in ΔESALs.

The differences in the curves are a result of two factors. The first is the magnitude of the effect that a variable multiplied by its coefficient has in comparison to the other terms in the model. The second factor is the variation for each variable within the dataset, i.e., the size of the standard deviation. Accordingly, a larger standard deviation causes greater variation in the curves.

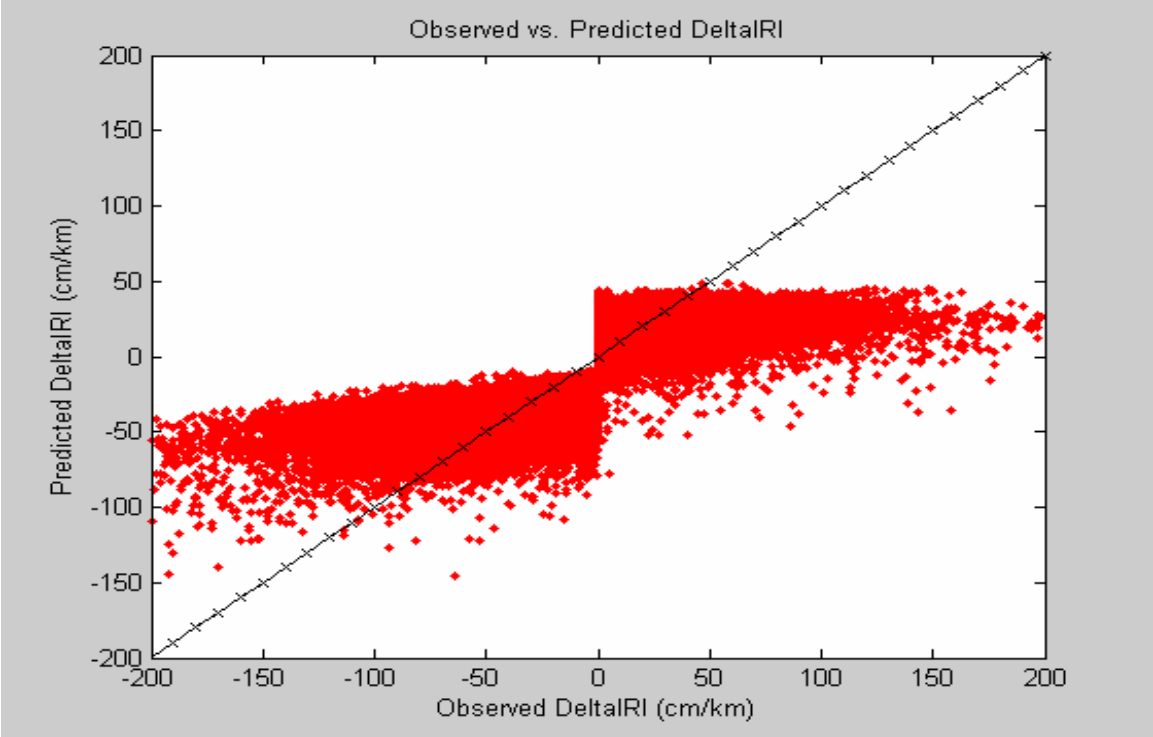

Figure 22: Observed vs. Predicted ΔIRI with outliers

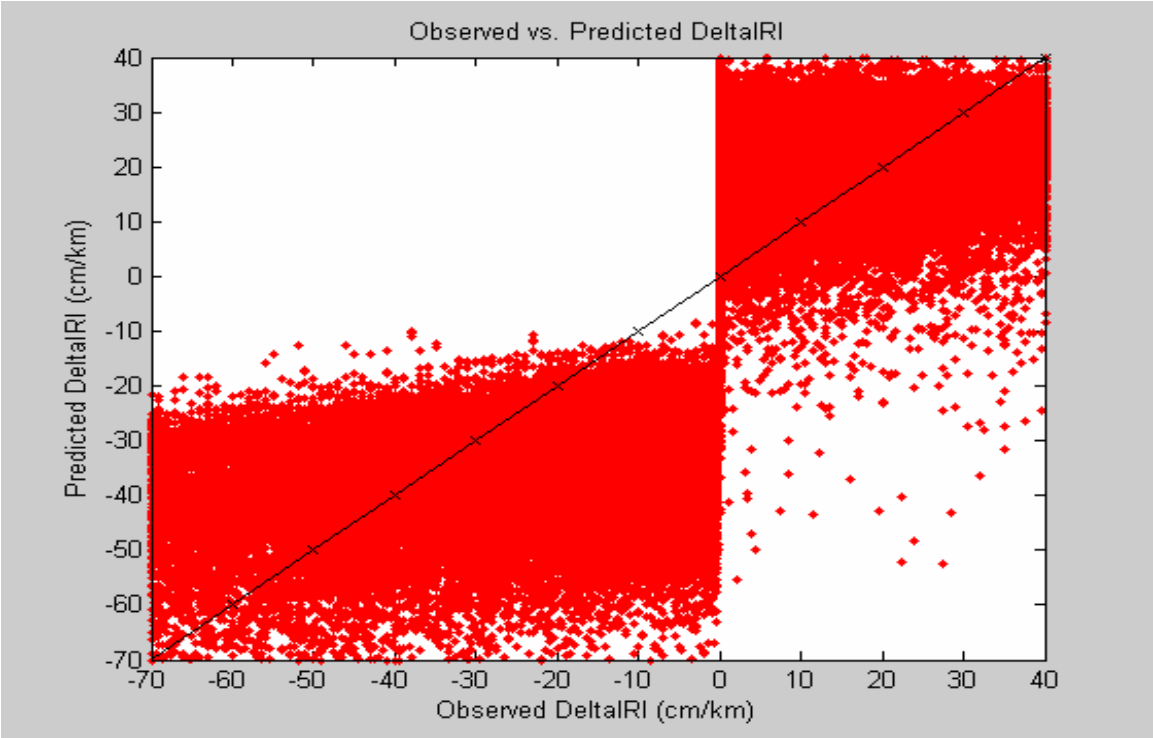

Figure 23: Observed vs. Predicted ΔIRI capturing the range in which the model does not underestimate or overestimate the dependent variable

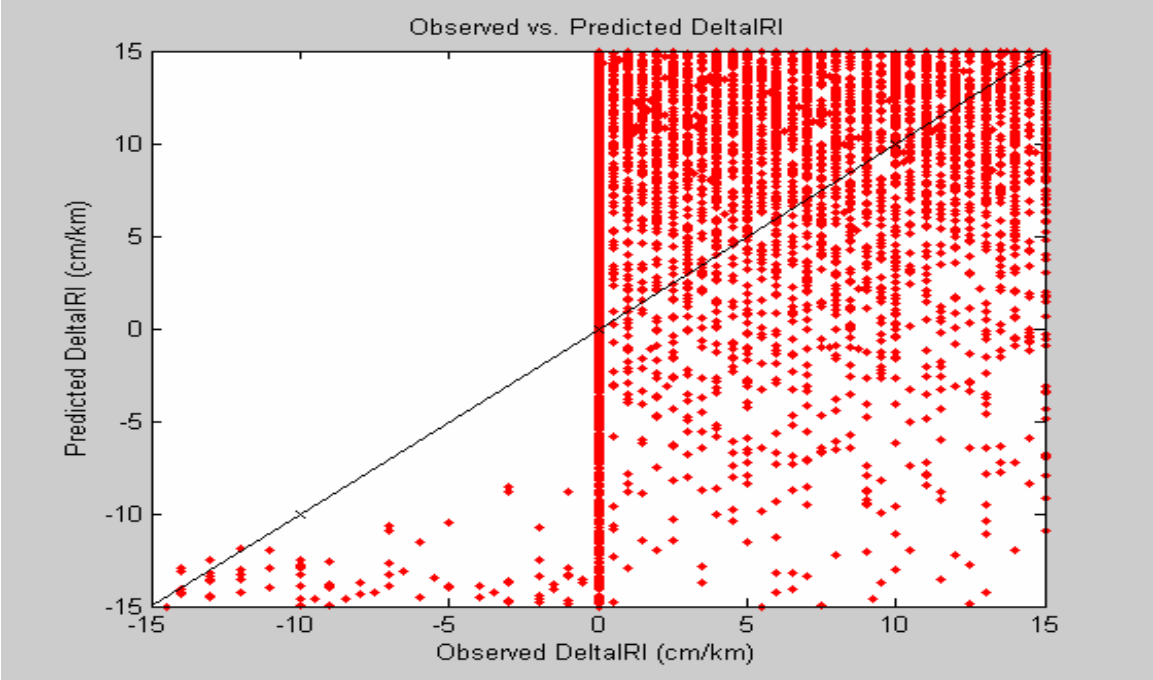

Figure 24: Observed vs. Predicted ΔIRI for the range where the model sometimes overestimates magnitude of the dependent variable

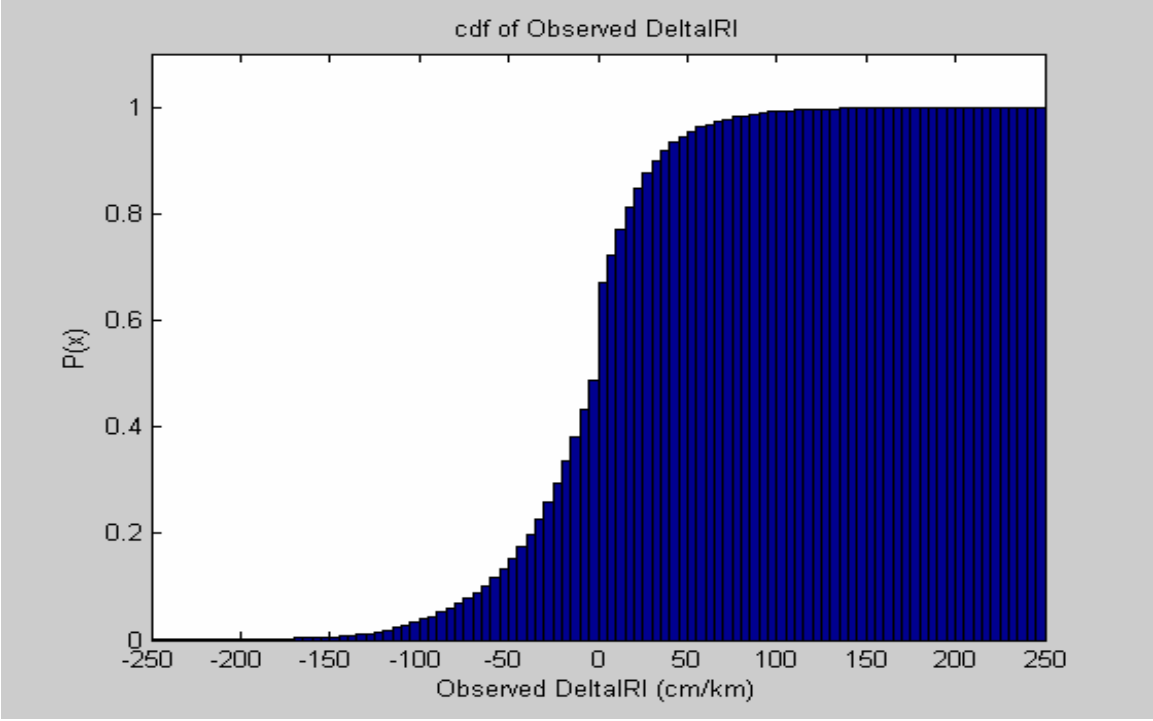

Figure 25: Cumulative Distribution Function for Observed ΔIRI for the half of the dataset that had been removed prior to model estimation and used in predictions

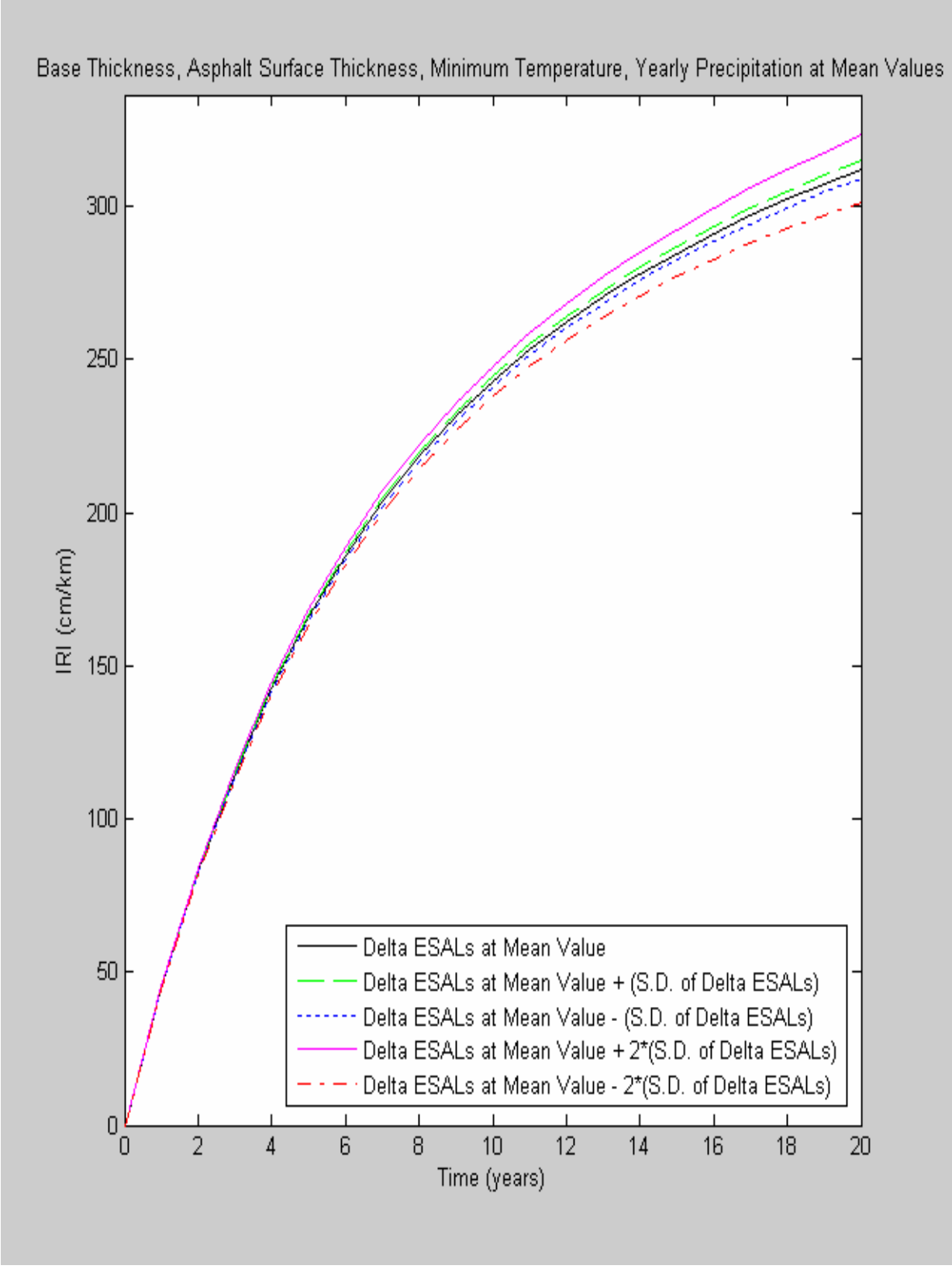

Figure 26: IRI deterioration curves with ΔESALs varied

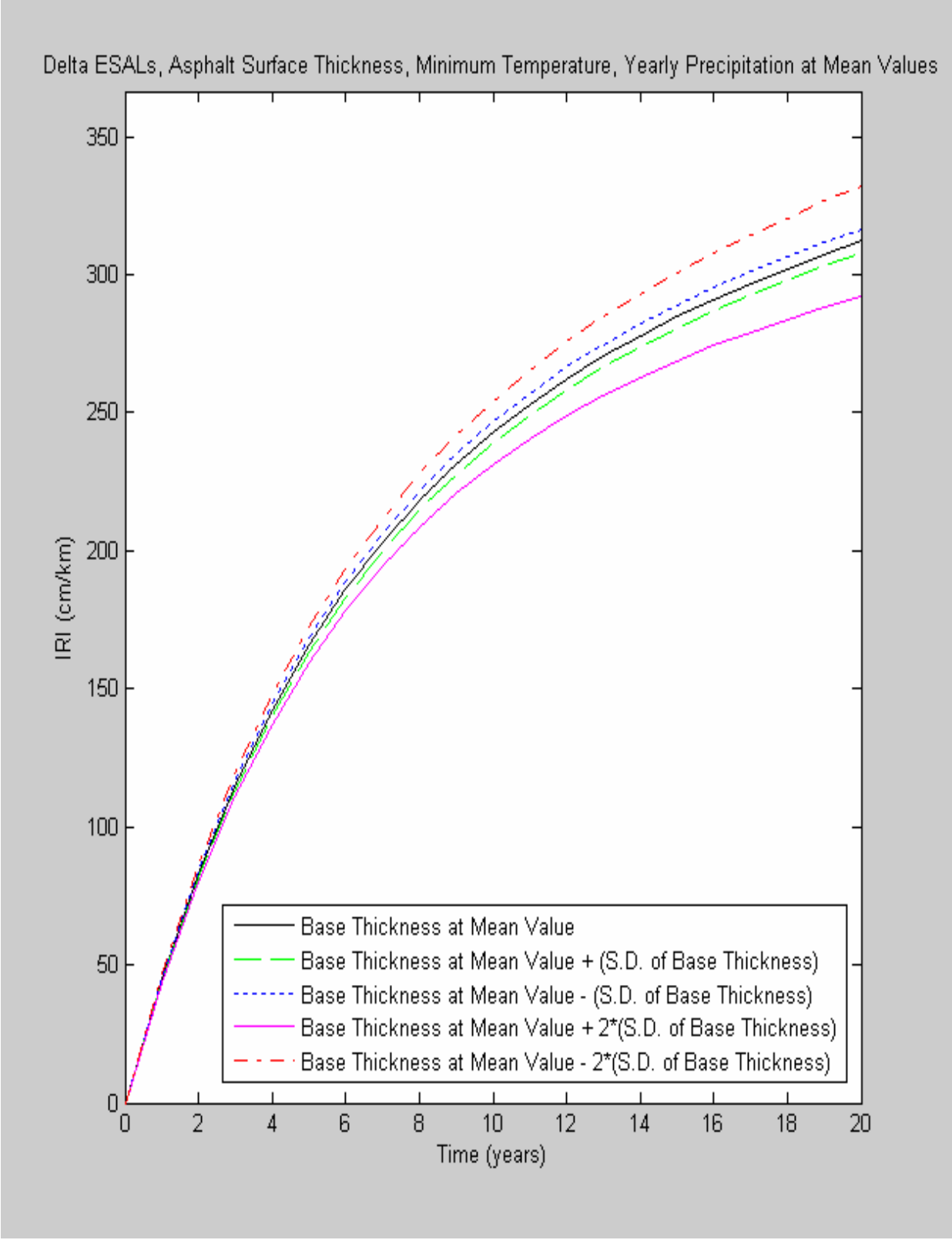

Figure 27: IRI deterioration curves with base thickness varied

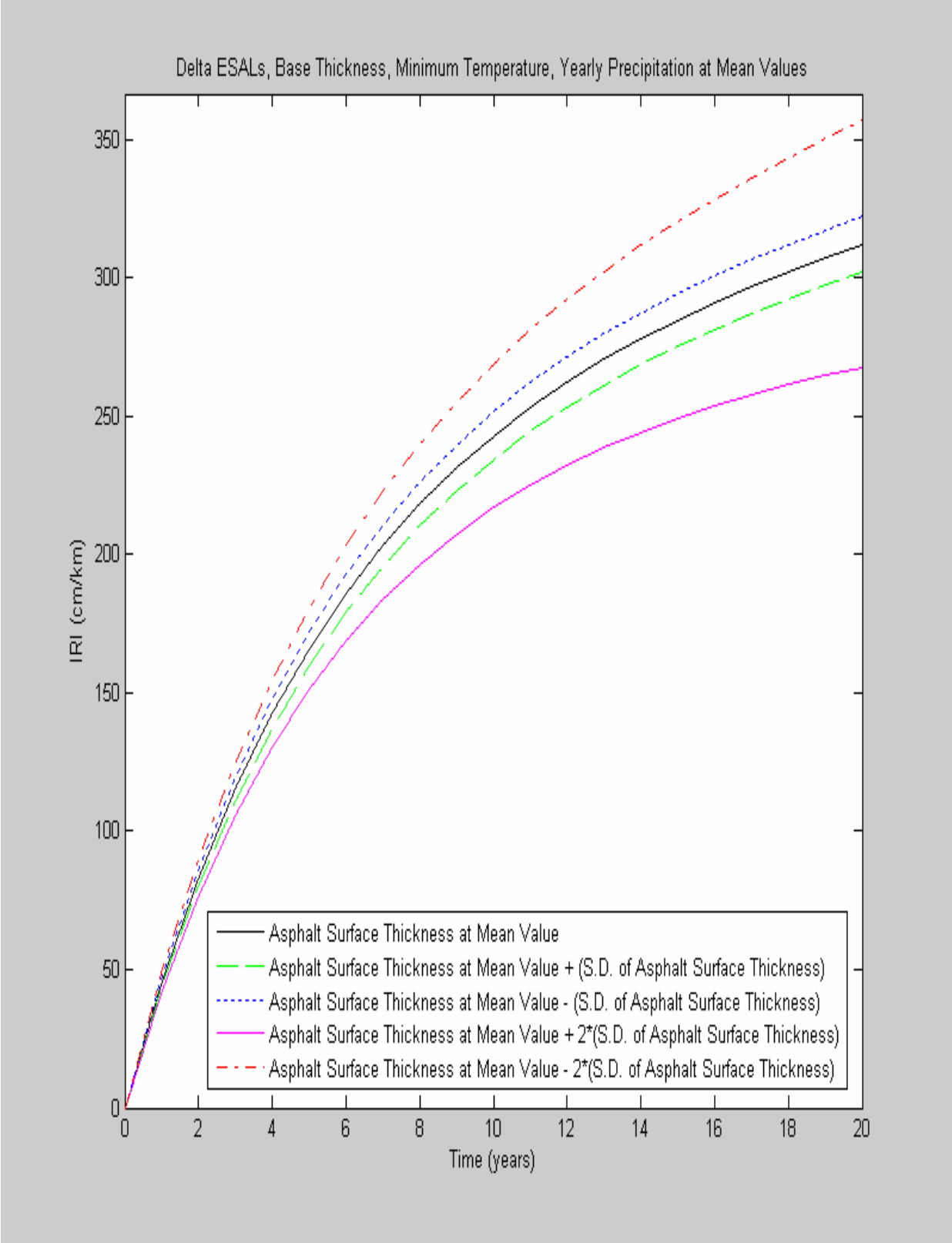

Figure 28: IRI deterioration curves with asphalt surface thickness varied

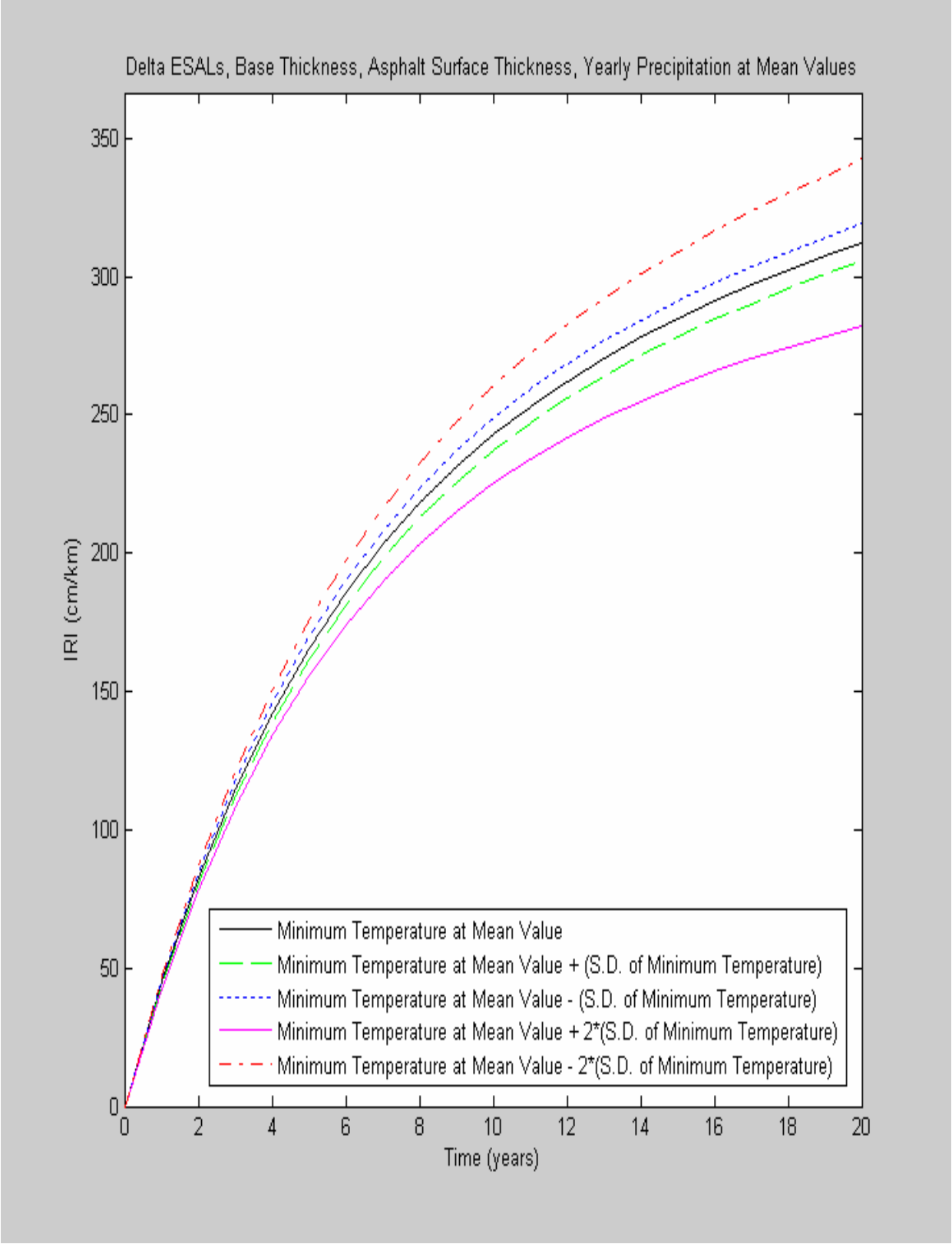

Figure 29: IRI deterioration curves with minimum temperature varied

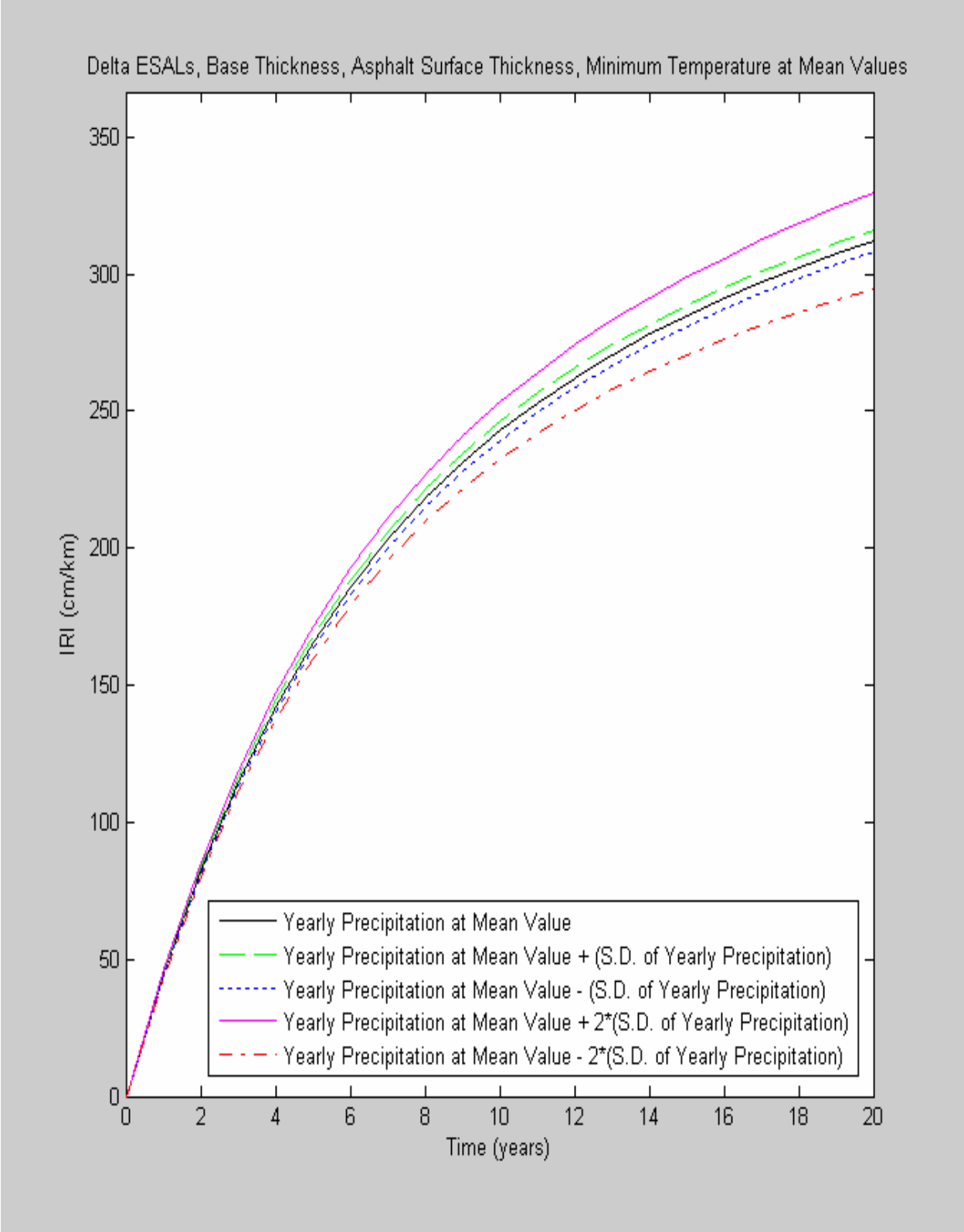

Figure 30: IRI deterioration curves with yearly precipitation varied

5.0 PORTLAND CEMENT CONCRETE PAVEMENT DETERIORATION

In contrast to the large data sets and rich information available for AC pavements, the WSPMS database contains only a small number of observations on PCC pavements. Furthermore the number of useful observations of them is even smaller they are "censored" observations: a large fraction consist of pavements for which the initiation of the distress of interest was not observed. As explained in Section 2.2, a censored observation occurs when only a bound is known on the time of failure. There are several types of censoring. Right censoring occurs when there is one or more pavement sections for which only a lower bound is known on the lifetime. Another form of censoring is left censoring. An example of left censoring is when a pavement section's failure occurs before the beginning of an observation period. Data can be both left- and right-censored if the conditions described above for the two types occur. In the WSPMS database, a large fraction of the condition data for PCC pavements is either left censored or right censored.

Given the small sample sizes and the prevalence of censoring in the PCC pavement condition data, it was not possible to develop statistically significant models of PCC pavement cracking initiation for either longitudinal or transverse cracking. Similarly, it was not possible to develop a meaningful model of IRI progression for PCC pavements.

Distributional analysis was performed using data in the WSPMS database for the Mean Time to Failure (MTTF), where failure was defined as the initiation of longitudinal and transverse cracking in portland cement concrete (PCC) pavements. Here, cracking initiation is defined as greater than zero percent of slabs cracked. In the longitudinal cracking analysis, 74 pavement sections are used, 38 of which are censored. For the data analysis of the transverse cracking data analysis, the number of pavement sections is 75 sections, 45 of which are censored.

Data summaries are given in Table 5 for the longitudinal cracking distribution**.**

Table 5: Characteristics of the Longitudinal Cracking Distribution

	Estimate	Standard Error
Mean (MTTF) (yrs.)	2.601	0.190
Standard Deviation	1.464	0.070
Median	2.4	0.201

It can be seen that the MTTF is unrealistically small. This is so because more than a third of the initiation times of longitudinal cracking for the PCC pavement sections (30 out of 74) are left-censored, and, as such, the MTTF for these sections appears to be zero, which biases the results reported in Table 5.

A similar distributional analysis of the transverse cracking data produced the results shown in Table 6.

Table 6: Characteristics of the Transverse Cracking Distribution

	Estimate	Standard Error
Mean (MTTF) (yrs.)	3.032	0.294
Standard Deviation	1.440	0.0656
Median	2.904	0.310

It should be noted that in most of the sections, cracking had occurred at the time of first observation or it did not appear at all over the set of observations, so a large fraction of the data is either left- or right-censored. The observed transverse cracking was never of great severity.

6.0 CONCLUSIONS

The major conclusions of this research can be summarized as follows.

1. The two performance models developed using the WSDOT PMS data for AC pavements or overlays (cracking initiation and IRI) are satisfactory.

2. The following explanatory variables were found to be the most relevant predictors of the number of ESALs-to-cracking initiation of overlays on AC pavements.
    - The overlay thickness
    - The type of AC mix used for the overlay
    - The thickness of the underlying AC layers prior to application of the overlay
    - The existing longitudinal and alligator cracking prior to application of the overlay
    - The base thickness and type (whether it was untreated, granular material, PC-treated, or AC-treated)
    - The maximum temperature during the hottest month and the minimum temperature during the coldest month (averages taken over the life of the overlay)
    - The number of freeze-thaw cycles and the average precipitation
3. The following explanatory variables were found to be the most relevant predictors of the annual increment in IRI for AC pavements and overlays.
    - The IRI in the previous year
    - The number of ESALs in the subject year
    - The cumulative number of ESALs prior to the subject year
    - The base thickness
    - The total thickness of AC (including all overlays)
    - The number of years since the last overlay or bituminous surface treatment
    - The type of the last MR&R activity applied to the pavement (overlay, BST or routine maintenance)
    - The minimum temperature in the coldest month (the average over the life of the pavement)
    - The annual precipitation (the average over the life of the pavement)
4. We were not successful in developing models using the WSDOT PMS data for PCC pavements (crack initiation and IRI). The main reason for this was

the small number of PCC observations available in the WSDOT PMS database.

5. This research has identified a list of variables recommended for collection by Caltrans. Other state DOTs currently collect elements of these variables. Appendix A provides a list of these variables.
6. To assist in making predictions using the model of cracking initiation for AC overlays, the research team developed a numerical integration procedure using Macros in *Microsoft Excel*. The description of this procedure appears in Appendix B.

Our main recommendations are:

1. To complete the AC Pavement Performance Model suite, a crack progression model should be developed. The progression model should be used jointly with the crack initiation model developed in this research.
2. The completed AC pavement models (crack initiation and progression, IRI progression) should be tested on California PMS data. These data can either be collected as part of a pilot project or drawn from the extant Caltrans' PMS database. (If the latter source is chosen, that database will need to populated with consistent information before testing the model.) If the results of the tests are positive, then Caltrans can essentially use these as temporary AC Pavement Performance models.
3. Once Caltrans has populated its PMS database with sufficiently extensive condition survey data, the models developed in this report can be updated with the California data by using statistical fusion procedures such as Bayesian Updating.
4. The ultimate objective of the development of such models is to use them within an integrated Pavement Management System. The models can provide predictions to support MR&R planning at both the project and network levels. Therefore, to fully reap the benefits of its investment in this research, Caltrans should continue its efforts at modernizing its Pavement Management System.

7.0 REFERENCES

1. AASHTO. *AASHTO Guide for Design of Pavement Structure.* American Association of State Highway and Transportation Officials, 1993.
2. Crowder, M.J. et al. *Statistical Analysis of Reliability Data.* Chapman and Hall, 1991.
3. Greene, W. H. *Econometric Analysis.* Macmillan Publishing Company, 1993.
4. Kalbfleisch, J.D. and Prentice, R.L. *The Statistical Analysis of Failure Time Data.* John Wiley and Sons, 2002.
5. Kay, K.R., et al. *Pavement Surface Condition Rating Manuel.* Washington State Department of Transportation, 1992.
6. Leemis, L. M. *Reliability, Probabilistic Models and Statistical Methods.* Prentice-Hall, 1995.
7. Mishalani, R. and Madanat, S. M. "Computation of infrastructure transition probabilities using stochastic duration models." *Journal of Infrastructure Systems.* 8 (4): 139–148. 2002.
8. Meeker, W. Q. and Escobar, L.A. *Statistical Methods for Reliability Data.* John Wiley and Sons, 1998.
9. Pindyck, R. and Rubinfeld, D. *Econometric Models & Economic Forecasts.* McGraw-Hill, 1981.
10. Shin, H. C. *Models of Crack Initiation and Progression for Asphalt Concrete Pavements.* Ph.D. dissertation, University of California, Berkeley, CA, 2001.
11. Stata Corporation. *Survival analysis and epidemiological tables,* Stata press publication, 2003.

8.0 APPENDIX A: LIST OF VARIABLES REQUIRED FOR THE CALTRANS PMS

The purpose of this chapter is to recommend variables that are important for modeling that should be included in the Caltrans PMS. These variables are divided into two parts: variables that are essential and variables that are useful, though not critical.

A.1. FIRST LEVEL OF PRIORITY: ESSENTIAL FOR MODELING

A.1.1. Condition Data for Rigid Pavements

Type: Faulting

Severity: Difference in elevation at the joint (mm). Extract from profilometer data.

Extent: Collect the sample of fault height within the section, either the entire section when collected with the profilometer or from a representative subsection of random sampling if not collected automatically. Report the average and standard deviation of fault heights within the section.

Type: Transverse Cracking

Severity: Cracked or not cracked (per slab)

Extent: Percentage of slabs cracked

Type: Longitudinal cracking

Severity: No cracks, one crack, or two cracks per slab

Extent: Percentage of slabs that have one crack in wheel path, percentage of slabs that have two cracks in wheel path; percentage of slabs that have one crack in centerline, percentage of slabs that have two cracks in centerline

Type: Corner cracking

Severity: 0, 1, 2, 3, 4 cracks per slab

Extent: Percentage of slabs with one, two, three, or four cracks

A.1.2. Condition Data for Flexible Pavements

Type: Alligator cracking

Severity: Combination of crack width and a qualitative measure

- Low: Branched, longitudinal, discontinuous thin cracks are beginning to interconnect and form the typical alligator pattern. There is no spalling along the cracks. A single, continuous crack may appear, usually along the wheel path, with frequent, intermittent smaller cracks running at angles to the primary crack.
- Medium: Cracking is completely interconnected and has fully developed an alligator pattern. Spalling appears at the edges of cracks. The predominant pieces formed by the cracking may be large ones (12 in. or more in the longest dimension). The cracks may be greater than 1/4 in. wide, but the pavement pieces are still in place.
- High: The pattern of cracking is well developed with small pieces (less than 12 in. in the longest length) predominating. Spalling is very apparent at the crack. Individual pieces may be loosened and may rock under traffic. Pieces may be missing. Pumping of fines up through the cracks may be evident.

Extent: Separate the alligator cracking measurements into the three severity types. Add together the lengths for each type in both wheel paths of the surveyed lane. Divide the accumulated lengths by twice the length of the segment (two wheel paths per lane).

Type: Longitudinal cracking

Severity: Width of the crack

Extent: The extent of longitudinal cracking is recorded as a percentage of the length of the surveyed segment. Separate the measurements for each type of crack severity, then

add together the length data for the surveyed lane. Divide the accumulated lengths by the length of the segment.

Note: The result for this measure may be greater than 100% if there are many parallel cracks.

Type: Thermal cracking

Severity: Width of crack

Extent: Percentage of section length with no cracking, and percentage of section length with cracking plus the distribution of crack spacing

Type: Rutting

Severity: N/A

Extent: Record the average rut depth in the wheel path and the standard deviation of the rut depths for the segment. This can be done automatically with vehicles using laser sensors. At least five sensors are needed: two outside of wheel paths, two in wheel paths, and one between wheel paths.

Type: Reflection cracking for AC/AC

Note: Flexible pavement crack types previously defined.

Type: Reflection cracking for AC/PCC or CTB (cement treated base)

	Transverse	Longitudinal	Corner
Severity:	Width	Width	Width
Extent:	Cracks per 100 m	Length	Cracks per 100 m

Type: Roughness

Severity: N/A

Extent: Measured and reported in units of IRI

A.1.3. Climate Data

- Rainfall: Total annual rainfall in mm
- Temperatures: Annual temperature distribution and daily air temperature change distribution

A.1.4. Traffic Data

- Monthly truck axle load distribution
- Monthly truck type distribution

A.1.5. Pavement Structures

- Subgrade soil type by Unified Classification System
- Total thickness of granular layer
- Total thickness of cemented soils
- Total thickness of portland cement concrete
- Total thickness of asphalt layers
- Thickness of overlay
- Visible maintenance activity type (qualitative description)

A.2. Second Level of Priority: Useful but Not Critical for Modeling

A.2.1. Condition Data for Rigid Pavements

Type: Joint spalling

Severity: The severity of joint spalling is quantified by the size of the spalls in the joints that are spalled.

- Low: 1/8-in. to 1-in. spalls
- Medium: 1-in. to 3-in. spalls
- High: Greater than 3-in. spalls

Example: A segment can have 20% low spalls, 15% medium spalls and 10% high spalls.

Extent: The extent of the joint spalling is quantified as the percentage of spalled joints out of the total number of joints in the segment.

Type: Crack Spalling

Severity: The severity of the crack spalling is quantified by the size of the spalls in the cracks that are spalled:

- Low 1/8-in. to 1-in. spalls
- Medium 1-in. to 3-in. spalls
- High Greater than 3-in. spalls

Example: a segment can have 20% low spalls, 15% medium spalls and 10% high spalls.

Extent: The extent of the crack spalling is quantified as the percentage of spalled cracks out of the total number of cracks in the segment.

Type: Pumping

Severity: Qualitative measure

- Low: Slight shoulder depression evident, little or no staining

- Medium: Moderate shoulder depression with obvious staining
- High: Severe shoulder depression and/or significant staining

Extent: The extent is quantified by the percentage of the number of joints and cracks in the segment that exhibit pumping.

Type: Patching

Severity: The severity of patching is quantified by a representative percentage of area of patch within a typical patched panel.

Extent: The extent of patching is quantified by the percentage of panels in a segment that have patches.

Type: Raveling or scaling

Severity: The severity of raveling or scaling is determined from personal judgment on the basis of the following descriptions.

- Slight: The aggregate or binder has started to wear away but has not progressed significantly. The pavement only appears slightly aged and slightly rough.
- Moderate: The aggregate or binder has worn away and the surface texture is moderately rough and pitted. Loose particles may be present, and fine aggregate is partially missing from the surface.
- Severe: The aggregate and/or binder have worn away significantly, and the surface texture is deeply pitted and very rough. Fine aggregate is essentially missing from the surface, and pitting extends to a depth approaching one half the size of the coarse aggregate.

Extent: The extent of raveling or scaling is the percentage of the surface area of the pavement that is raveled or scaled.

Type: Blowups

Severity: N/A

Extent: The number of occurrences in the segment are counted and recorded.

Type: Wear

Severity: N/A

Extent: Record the average wear (rut) depth in the wheel path and the standard deviation of the wear depths for the segment or for a sample. This can be done automatically with vehicles using laser sensors. At least five sensors are needed: two outside of wheel paths, two in wheel paths, and one between wheel paths.

A.2.2. Condition Data for Flexible Pavements

Type: Flushing, bleeding

Severity: Qualitative measure

- Low: Minor amounts of the aggregate have been covered by excess asphalt, but the condition has not progressed significantly.
- Medium: Significant quantities of the surface aggregate have been covered with asphalt. However, much of the coarse surface aggregate is exposed, even in areas that show flushing.
- High: Most of the aggregate is covered by asphalt in the affected area. The area appears wet and is sticky in hot weather.

Extent: Percentage of wheel path

Type: Raveling

Severity: Qualitative measure

- Low: The aggregate or binder has started to wear away but has not progressed significantly. The pavement only appears slightly aged and slightly rough.

- Medium: The aggregate or binder has worn away and the surface texture is moderately rough and pitted. Loose particles may be present, and fine aggregate is partially missing from the surface.
- High: The aggregate and/or binder have worn away significantly, and the surface texture is deeply pitted and very rough. Fine aggregate is essentially missing from the surface, and pitting extends to a depth approaching one half the size of the coarse aggregate.

Extent: The extent of raveling is estimated and expressed as a percentage of the surface area of the segment.

Type: Patching

Severity: N/A

Extent: Percentage of area of segment

Type: Pavement edge

Severity: Pavement edge is further broken down into three categories:

- Edge raveling: This occurs when the pavement edge breaks away from roadways without curbs or paved shoulders.
- Edge patching: Edge conditions can still occur with paved shoulders, and edge patching is the repair of this condition.
- Lane less than 10 feet: This indicates that the edge raveling has progressed to the point where pavement width from the center line to the outer edge of roadway has been reduced to less than 10 feet.

Extent: Percentage of lane length

Type: Block cracking

Severity: The severity of block cracking is defined by the average size of the blocks *and* the average width of the cracks that separate them.

Block size:

- Low: 12-ft. x 12-ft. blocks (9x9 and larger)
- Medium: 6-ft. x 6-ft. blocks (5x5 to 8x8)
- High: 3-ft. x 3-ft. blocks (2x2 to 4x4)

Crack size:

- Low: Less than 1/4 inch
- Medium: Over 1/4 inch
- High: Spalled

Extent: Percentage of area of segment

Type: Corrugations

Severity: Qualitative measure

- Low: Caused some vehicle vibration, which creates no discomfort
- Medium: Causes significant vehicle vibration, which creates some discomfort
- High: Causes excessive vehicle vibration, which creates substantial discomfort and/or vehicle damage requiring a reduction in speed

Extent: Percentage of extent of segment length

Type: Delamination

Severity: N/A

Extent: Record the number and locations in a segment

Type: Potholes

Severity: Pothole area and pothole depth (average in segment):

- Small: Less than 1.0 ft. (0.30 m) square
- Medium: Between 1.0 ft. (0.30 m) and 3.0-ft (0.91-m) square
- Large: Greater than 3.0-ft. (0.91 m) square

Extent: Report number of potholes in a segment.

Type: Shoving (slippage)

Severity: N/A

Extent: Note the size of the area in a segment.

A.2.3. Climate Data

- Wind: Wind speed distribution
- Clouds: Cloud cover distribution
- Humidity: Relative humidity

A.2.4. Traffic Data

- AADT (Average Annual Daily Traffic)
- Daily truck axle load distribution
- Daily truck type distribution
- Speed (daily speed distribution)

A.2.5. Pavement Structures

- Material type of overlay
- Maintenance surfacing type:
  - Fog seal
  - Slurry seal
  - Chip seal
  - Sand seal
  - Microsurfacing
- Geometric (distribution of vertical grade): check if possible to collect it by profilometer.
- Construction quality: If dense graded asphalt, measure percentage air void of overlay (distribution).

A.2.6. Additional Pavement Structure Data for PCC Pavements

- Check for dowels or no dowels
- Check if it is CRC (continuously reinforced).

Note: Additional condition survey procedures should be developed for CRC.

- Check if tied concrete shoulder, AC shoulder, or wide truck lane.

9.0 APPENDIX B: NUMERICAL COMPUTATION OF THE EXPECTED CUMULATIVE ESALS-TO-CRACKING INITIATION

This appendix describes the numerical integration procedure used to predict the expected number of ESALs-to-cracking initiation of AC overlays placed on AC pavements. This numerical procedure can be used in conjunction with the model described in Chapter 3.

As explained in Chapter 3, the stochastic Duration Model for predicting ESALs to overlay cracking initiation is a semi-parametric (Cox) model. In a Cox Model, the baseline hazard function is a not a parametric distribution but an entirely empirical one. Therefore, unlike a parametric model such as the Weibull Model, the Hazard Rate Function does not have a closed-form expression that can be integrated in order to compute the expected ESALs-to-cracking. Instead, we developed a numerical integration procedure that is described herein.

The data includes n observations, so we have *n* rows in *Excel*. For every observation, we have values for the cumulative ESALs to failure , *t,* and values for the different explanatory variables $\underline{x}$ (Tmin, Tmax, overlay thickness, etc.). Assume for simplicity that we have one explanatory variable, *x.*

Let column A include all the values of *t* (*n* rows) and Column B include all the values of *x* (*n* rows, as well).

After estimation of the model, the econometric software *Stata 8* gives us a value of S_0 for every value of *t.* Thus we have an extra column C that includes the values of S_0 (*n* rows, as well).

For every value of x, we have a distribution of the cumulative ESALs to failure *t.* So given *x,* the expected cumulative ESALs to failure is given by:

$$\overline{E}[t/x] = \sum_{t=0}^{\infty} S(t)\Delta t = \sum_{t=0}^{\infty} {S_0}^{\Psi(x)}\Delta t \qquad \textbf{(B.1)}$$

where t is the cumulative ESALs to failure, S_0 is the base survival function, and $\Psi(x) = e^{\beta x}$.

For every *x,* there is one value of *Ψ(x),* let column D include the *n* values of *Ψ(x).* The upper bound of the expected value of t given x is calculated using the equation:

$$\overline{E}[t/x] = \sum_{i=0}^{n-1} S_{0,i}{}^{\Psi(x)}(t_{i+1} - t_i) \qquad \textbf{(B.2)}$$

where i=1 corresponds to the first row of the data, $t_0 = 0$, $S_{0,0} = 1$, and $\overline{E}[t/x]$ is the upper bound of the expected value of t given x.

The lower bound of the expected value of t given x is calculated using the equation:

$$\underline{E}[t/x] = \sum_{i=0}^{n-1} S_{0,i+1}{}^{\Psi(x)}(t_{i+1} - t_i) \qquad \textbf{(B.3)}$$

where i=1 corresponds to the first row of the data, $t_0 = 0$, $S_{0,0} = 1$, and $\underline{E}[t/x]$ is the lower bound of the expected value of t given x.

The expected value of t given x is thus the arithmetic mean of the results of equations B.2 and B.3 and is given by:

$$E[t/x] = \frac{\overline{E}[t/x] + \underline{E}[t/x]}{2} \qquad \textbf{(B.4)}$$

Note: The observations that are right censored are excluded form the sample for prediction. (They are only used for the estimation of the parameters of the model).

Equations B.2 and B.3 are simple to compute and one does not need a computer program to calculate them. However, in order to calculate the expected value for every value of x in the data, two *Excel* macros were written to compute equations B.2 and B.3. The two programs are very similar; the differences are the underlined parts of the programs below.

9.1 Program for equation B.2

```
Number of first row = 1
Number of last row = n
Number of first row of x = 1
Number of last row of x = n
Column A = 1
Column C = 3
Output Column E =5

For j = Number of first row of x  To Number of last row of x
s = t1 ….Note: this corresponds to the value of equation 2 for i=0
         For i = Number of first row To number of last row
s = s + (Cells(i+1, Column A) - Cells(i , Column A)) * (Cells(i, ColumnC)) ^
(Cells(number of first row of x, Column D))
           Next i
Cells(j, Output Column E) = s
Next j
End
```

The output of this program will be the upper bound of the expected value of *t* for every value of *x,* and will appear in a column E.

9.2 Program for equation B.3:

```
Number of first row = 1
Number of last row = n
Number of first row of x = 1
Number of last row of x = n
Column A = 1
Column C = 3
Output Column F =6
For j = Number of first row of x  To Number of last row of x
s = t1 ….Note: this corresponds to the value of equation 2 for i=0
         For i = Number of first row To number of last row
s = s + (Cells(i+1, Column A) - Cells(i , Column A)) * (Cells(i+1, ColumnC)) ^
(Cells(number of first row of x, Column D))
           Next i
Cells(j, Output Column F) = s
Next j
End
```

The output of this program will be the lower bound of the expected value of *t* for every value of *x,* and will appear in a column F.